FINITE DIFFERENCE SOLUTION OF WAKES FOR TURBULENT FLOW BEHIND A FLAT PLATE

by

Md. Tazul Islam

A thesis

Submitted to the Department of Mechanical Engineering in partial fulfilment of the requirements for M.Sc.Engg. (ME) degree.

Bangladesh University of Engineering and Technology
Dhaka. July, 1986.

Approved as to Style and Contents by:

(Dr. S.M. Nazrul Islam) — Chairman
Professor
Department of Mechanical Engineering
BUET, Dhaka.

(Dr. M.H.Khan) — Member
Professor and Head
Department of Mechanical Engineering
BUET, Dhaka.

(Dr. D.K. Das)
Professor
Department of Mechanical Engineering — Member
BUET, Dhaka.

(Dr. M.Q. Islam) — Member
Associate Professor
Department of Mechanical Engineering
BUET, Dhaka.

(Dr. A. Halim) — External Member
Professor
Department of Water Resources Engineering
BUET, Dhaka.

July, 1986

ABSTRACT

The present investigation was on the mean flow parameters of the wake, identifying the initial conditions and a suitable turbulent shear stress model. The equations for mass and momentum conservation for turbulent flow were solved numerically by using appropriate boundary conditions. Finite difference scheme was used to solve the above equations. The calculations were performed for Reynolds number, Re θ e=2. $18X10^3$, $2.01X10^3$, $1.9X10^3$ and $1.7X10^3$ for which the flow may be assumed to be turbulent. Mean properties of the flow at the trailing edge were expressed by a empirical relation using the experimental values of Faruque [8]. Prandtl's mixing length was expressed as a function of shear layer thickness and it was used in the turbulent shear stress model.

Within the wake near the trailing edge of the plate the transverse velocity gradient was high. The velocity gradient decreases with increse of axial distance from the trailing edge of the plate. The momentum thickness increased with the increase of Reynolds number. The center-line velocity increased with the increase of axial distance. The rms deviation of mean flow from self-preserving flow, decreased gradually with the increase of axial distance. The rms deviation became less and the velocity profile became self-preserving earlier for high Reynolds number.

Drag Co-efficient increased with the increase of Reynolds number.

The calculated results have also beencompared with the available experimental results. Most of them are in close agreement with experimental results.

ACKNOWLEDGEMENTS

With deep sincerity, the author expresses his profound indebtedness to Professor S.M. Nazrul Islam, Department of Mechanical Engineering, BUET, Dhaka for his guidance, encouragement and invaluable suggestion in achieving every minute detail of this thesis.

The author is highly grateful to Professor M.H.Khan, Professor M. Abdul Halim, Professor Dipak Kanti Das, Dr. M. Wahhaj Uddin and Dr. M.Q. Islam for their constructive criticism and invaluable suggestions which have definitely raised the quality of the work.

He is also indepted to P.K. Md. Omar Faruque who assisted him various ways at every phase of the work.

He is also indebted to Computer Center, BUET, for providing facilities without which this computational work would not have been possible.

Finally, the author wishes to thank Mr. Abdus Samad for typing the thesis with patience and care.

TABLE OF CONTENTS

LIST OF FIGURES

LIST OF TABLES

LIST OF APPENDICES

NOMENCLATURE

A, A_1	Constants
A_τ	Turbulent Mixing Coefficient
a, a_2	Constants in Empirical Equations
B, B_1	Constants
b	Width of Wake
Bx, By, Bz	Body Forces per Unit Mass along the x, y and z Direction.
c	Constant
Cdm	Drag Co-efficient (Without Pressure Gradient)
Cd	Drag Co-efficient (With , Pressure Gradient)
D	Plate Thickness
D_1	Drag per Unit Depth
f	A Function of η
g	Acceleration due to Gravity
H	Shape Factor
H_1, H_2	Small Increments of Length in Axial and Transverse Direction.
K	Kinetic Energy
K_2, K_3	Constants
L	Characteristic Body Dimension
ℓ	Prandtl's Mixing Length
M	Momentum Defect per Unit Time and Depth
n	Power Index
n_1	Constant
p	Mean Static Pressure
p^o	Instantaneous Static Pressure
p'	Fluctuating Static Pressure

Red	Reynolds Number Based on Diameter
Re Θe	Reynolds Number Based on the Momentum Thickness and Average Velocity
t	Time
t^o, t'	Instantaneous and Fluctuating Components of Time
u^o, v^o, w^o	Instantaneous Velocities in x,y and z Direction Respectively
u', v', w'	Fluctuating Velocities in x,y and z Direction Respectively
u	Axial Mean Velocity
U	Non-Dimensional Mean Axial Velocity, u/u_∞
u_∞	Free-Stream Velocity
u^*	Shear Velocity
v	Transverse Mean Velocity
V	Non-Dimensional Mean Transverse Velocity v/u_∞
Y_G	Effective Width of Shear Flow
x,y	Co-ordinate System
X,Y	Dimensionless Axial and Transverse Distances $(xu_\infty/\nu \ , \ yu_\infty/\nu)$
ε_τ	Eddy Kinematic Viscosity
ε_1	Constant
α_1, α_2	Constants
δ	Boundary Layer Thickness
δ^*	Displacement Thickness
ε	Turbulent Energy Dissipation Rate
ν_t	Turbulent or Eddy Diffusivity
ν	Kinematic Viscosity
η	Self-Preserving Variable
ρ	Mean Density

μ	Absolute Viscosity.
ρ°, ρ'	Instantaneous and Fluctuating Components of Density.
χ	Constant used to Define Prandtl's New Formula.
λ_s	Proportionality Constant
$\tau_{xy}, \tau^{\circ}_{yz}, \tau^{\circ}_{zx}$	Instantaneous Shear Stresses in Different Direction
$\tau_{xx}, \tau^{\circ}_{yy}, \tau^{\circ}_{zz}$	Instantaneous Normal Stresses in Different Direction

Subscripts

c	Center-Line
i,j	Grid Indices Corresponding to x and y Direction Respectively
rms	Root Mean Square
av	Average
0	Trailing Edge
$\bar{A}$	Time Average
max	Maximum
min	Minimum

CHAPTER - I

INTRODUCTION

1.1 General

A wake is formed behind a solid body which is being towed through a fluid at rest or behind a solid body which has been immersed in a stream of a fluid. The velocities in a wake are lower than those in the main stream. A continuous exchange of momentum takes place in the wake from the high velocity region to the low velocity region. The change of velocity in a wake for incompressible flow is due to the loss of momentum caused by the drag on the body. The magnitude of difference of momentum between the wake and free-stream region determines the level of exchange of momentum. Typically high level of momentum exchange together with the fluid properties makes the flow to be turbulent. The wake generated with such turbulent flow is said to be turbulent wake.
The spread of the turbulent wake increases and the difference between the momentum in the wake and that out side becomes smaller with the axial distance from the body. The characteristic features of such wake flow are important for many practical applications. Such turbulent wakes are simple in nature but contain many features of turbulent shear flow. The researchers are being more attracted to work in this area.

1.2 Formation and Degeneration of Wake

When a fluid in motion separates from a surface and shears with another fluid having lower velocity forms two layers of different momentum. Such difference causes an exchange of momentum to form a shear layer. The geometry of the shear layer and the flow characteristics of the shear layer determine the loss of momentum and energy due to wake. The flow in the shear layer may be with or without pressure gradient. The shear layer is said to be free shear layer if it is not obstructed by boundaries. In case of free shear layer the fluid in contact with the outer boundary of the wake folds back into the surroundings, after separating from the surface. This folding engulfs the surrounding fluid and forms a ring vortex core which rolls downstream. After one or two revolutions, the vortices interact strongly with the other vortices and break down into turbulent eddies, [1]* if they originate from turbulent boundary layers. The interactions of turbulent eddies cause large scale vortical motion ; small scale vortical motions also evolve through breakdown of the large eddies.

The general character of the turbulent wake with shear layer is depicted in Fig. 1.1 with a dip in the velocity profile. The width of the wake increases and the dip in the velocity profile gradually levels off with distance from the body.

---

* Number in the parentheses indicate references.

1.3. Self-Preservation of Wakes

A large scale vortical motion is formed in the near region and a small scale vortical motion is evolved through breakdown of the large eddies in the far region of the wake. The small eddies contain less energy and they are invariant to mean and turbulent stress in the field. From the physical view point, the flow is said to be self-preserving when the eddies are invariant. The eddies are invariant when it has the capability to readjust with its surrounding eddies if it is subjected to any change in any property. For self-preserving flow field, the velocity scale, $(u_\infty - u_c)$ and length scale, ℓ_1 for two-dimensional wake, may be expressed as follows [11];

$$(u_\infty - u_c) = A_1 x^{-1/2} \; ; \; \ell_1 = B_1 x^{1/2}$$

where, A_1 and B_1 are constants.

An analytical solution of the governing equations may be obtained by using self-preserving laws. It is identified by Keffer [11] and keffer [12] that the mean quantities achieve self-preservation earlier in the flow than the turbulent quantities. Experimental results of Keffer [12] shows that all measured turbulent and mean quantities within wake are fully self-preserving beyond x/D=500.

1.4 Scope of Application

The flow near the trailing edge of an airfoil is considerably interesting from the view point of its design and application. The wake behind a flat plate is a limiting case of an airfoil. Wakes behind any obstacle are common in many engineering applications requiring special attention. The wakes in fluid machineries, motor vehicle, drilling technology, heat exchangers, cooling towers, cooling devices, control devices etc. are common features. A maneuvering air craft or submarine which is accelerating or decelerating leaves behind it a momentum defect in the form of jet or wake when it changes speed. All such wakes are turbulent in character and those need to be studied for drag and other parameters. Some experimental as well as theoretical works are available in this area.

1.5 Statement of the Problem

The flow development within the turbulent wake behind a flat plate has been studied numerically by developing computer program. The objectives of the present study are:

1. Identification of the initial condition of the wake. The initial velocity profile will be taken either from empirical formula or from any integral solution.

2. Finite difference formulation of the continuity and momentum equations. Development of computer program in order to solve those equations for mean velocity, momentum thickness, drag Co-efficient etc.

3. Identification of a suitable shear stress model for turbulent flow to fit the solution.

4. Comparison of the results to be obtained by calculation with the existing experimental results.

5. Study of the variation of drag coefficient and wake geometry for different Reynolds number.

6. Study of the self-preservation of the mean velocity in the developing region.

CHAPTER - II

LITERATURE SURVEY

2.1 General

The increasing availability of faster and more economical digital computers has stimulated the development of effective differential calculation methods. These methods predict quite accurately the most important features of many turbulent flows. The success in case of wall boundary layers is most striking. For this case the Prandtl mixing-length has led to predictions which agree well with experimental data over a wide range of conditions.

The prediction of properties in free shear flows was most commonly done by integral methods. But now the differential methods have become the center of interest with most researchers. A study of the proceedings of the 1968 Stanford Conference on computation of turbulent boundary layers, the proceedings of the 1972 Langlely working conference on free turbulent shear flows and the proceedings of the 1978 Imperial College second symposium on turbulent shear flows will provide an indication of the shift in the emphasis on differential method.

Turbulent flows can be expressed mathematically by the conservation of mass equation and the Navier-Stokes equations. Since the Navier - Stokes equations are non-linear, solution for each individual flow pattern has certain unique characteristics that are associated with its

initial and boundary conditions. The equations have been analysed by researchers for various flow pattern. But it is still not possible to make quantitative prediction concerning turbulent quantities without relying greatly on empirical data because in the time - averaged turbulent equations, there are more unknown dependent variables than the number of equations. In order to obtain the solution, it is necessary to make appropriate assumptions concerning the flow. These assumptions are based on physical concepts developed from experimental data and experience. In this way, many authors have developed empirical and semi-empirical equations to obtain a set of closed equations. Progress in this line of research (both theoretical and experimental) as related to turbulent wakes by various authors is presented in this chapter with their findings and conclusions. The term wake is commonly applied to the region of non-zero vorticity on the down stream side of a body immersed in a flow. In the turbulent wake the effects of the molecular viscosity is negligible, and it is turbulent from the trailing edge of the wake if it is generated by turbulent boundary layer at the beginning of the wake.

2.2 Experimental Investigation

Chevray and Kovasznay [13] investigated two-dimensional wake behind a thin flat plate mounted in the low speed wind tunnel. Measurements were taken with a single channel constant temperature hot-wire anemometer both for mean velocity and for turbulence. Reynolds number

based on boundary layer thickness, δ was $\frac{\delta u}{\nu} = 1.5 \times 10^4$ for all investigations. The boundary layer thickness and momentum thickness at the exit were 5.5 cm and 0.58 cm respectively. Using the experimental values of mean velocities the authors calculated the corresponding momentum thickness and the width of the wake. The flow in the wake was found approximately similar except close to the trailing edge. It was shown that the flow achieved approximate self-preservation at a distance $X/\theta_o = 300$ and exact self-preservation might occur at a distance where the shape factor H, tends to unity. It is to be noted here that the trailing edge turbulence level was not mentioned.

Hiroshi and Kuriki [14] experimentally studied the mechanism of transition in the wake of three thin flat plates of different dimensions. The plates were placed parallel to a uniform flow at subsonic speeds. The maximum thickness of the three plates were 0.3 mm and 3 mm respectively and the Reynolds number based on length of the plates ranged from 6×10^4 to 4×10^5. For the measurement of the mean velocity distribution, both fine Pitot - tube and hot-wire anemometer were used. At the trailing edge, parameters such as boundary layer thickness, displacement thickness and shape factor were not calculated by the authors [14]. They classified the transition region into three subregions viz. linear, non-linear and three-dimensional. In the two-dimensional (linear and non-linear) region the center-line velocity was found to vary exponentially. In the three-dimensional region it was approximately linear. From the velocity distribution curves the authors showed

that until x=30 to 40 mm, the distribution varied slowly, while a sharp increase of center-line velocity was found from x=40 to 60 mm. The experimental values of the mean velocities were found to fit to the empirical equation

$$\frac{u}{uo} = 1 - \frac{uo-u_c}{uo} \exp\left(a(y/y_{1/2})^2\right) \qquad (2.2.1)$$

Where, a = 0.69315.

The theoretical mean velocity distribution for a fully developed laminar wake of the above form and the experimental data were in good agreement with each other. However, they did not mention variation of the momentum thickness and the width of the wake in the axial direction. As the exit condition is laminar the development of the wake is not similar to that obtained by Chevray and Kovasznay [13].

Gartshore [17] investigated the two-dimensional wake of a square (0.635 cm) rod at adverse pressure gradients and at the pressure gradient for exact self-preservation. The velocity ratio $(u_\infty - u_c)/u_\infty$ was maintained approximately constant after $x/d_1 = 50$, the flow through wake having Reynolds numbers 6300 and 7300 based on the conditions at the trailing edge.

Keffer [11] investigated the wake produced by the two-dimensional cylinder of diameters 1.27 cm, 0.793 cm and 0.476 cm with straining the flow. The tunnel speed was held constant at 5.48m/sec so that the corresponding Reynolds number based on cylinder diameters were 4630, 2890 and 1740 for cylinder diameters 1.27 cm, 0.793 cm and 0.476 cm respectively. The mean quantities were measured with a Pitot

static tube. Keffer [11] found that the wake width increased exponentially with distance downstream. The mean velocity distribution of the wake profile was in no way self-preserving.

Schlichting's [15] work, which is mentioned in this section is devoted to an experimental investigation of the flow in the wake of a two-dimensional body. The experiments were conducted within a wind tunnel at a speed of about 50m/sec, Reynolds number based on the diameter was $Re_d = ud_1/\nu = 2.38 \times 10^4$. He found that the half-width of the wake varied parabolically and the center-line velocity defect varied exponentially. Experimental values of mean velocities were found to fit to the empirical equation

$$\frac{u_\infty - u}{u_\infty - u_c} = (1 - \eta^{3/2})^2 \qquad (2.2.2)$$

Where, $\eta = y/b$, b is the width of the wake and y is the vertical distance from the wake centerline. Schlichting's experimental results did not indicate the initial boundary layer parameters. These results agree satisfactorily with wake generated with a very thin boundary layer on the plate, but it may deviate from the results with thick boundary layer over the plate.

Hall and Hislop [16] investigated the velocity and temperature distributions in the turbulent wake behind a heated body of revolution. They found that the experimental values of the mean velocities fitted satisfactorily with

the empirical equation given by Schlichting [15] in equation (2.2.2). Swain [18] also obtained in a similar manner such an expression for the velocity profile in an axially symmetrical wake. The dimensionless profile of the velocity defect was obtained experimentally by Reichardt [19] in the wake behind a heated wire at a distance of $x=100\ r_o$ (r_o is the radius of the wire) from it. Similar experiments were also done by Fage and Falkner [22] in the wake behind a heated prismatic rod at a distance of $x=72\ r_o$ from it. The attempt of Goldstein [20] and other students of Taylor to apply the vorticity transfer theory for determining the velocity profile in an axially symmetric wake did not lead to results which agree with experimental data.

Faruque [8] investigated two-dimensional turbulent wakes formed behind thin flat plates mounted in a straight subsonic wind tunnel of suction type. The wind tunnel was originally designed and constructed by Islam [23] and installed by Khalil [24] . Two flat plates of different thicknesses , 1.905 cm and 1.27 cm were used for generating the wakes , at four different exit Reynolds numbers, i.e $Re\theta e = 2.18\times10^3$, 2.01×10^3, 1.9×10^3 and 1.7×10^3. The boundary layers were turbulent at the trailing edge of the plate, and the wakes formed with these boundary layers were assumed to be turbulent from the exit. The initial boundary layer was identified to be turbulent on the basis of the experimental values of velocities, which fitted to the universal velocity profile of turbulent boundary layer:

$$u^+ = B\log y^+ + A \qquad (2.2.3)$$

where, $u^+ = u/u^*$, $y^+ = u^* y/\nu$ and B and A are constants.

The velocity distribution in the neighbourhood of the flat plate was unstable due to the presence of high velocity gradient in the axial direction and instability decreased to make the flow self-preserving. The flow was not found to be self-preserving within the axial distance covered in the present investigation i.e. x/D = 56. The axial variation of half-width of the wake was approximately linear except close to the trailing edge, which was in agreement with the experimental results obtained by many investigators. The flow within the wake did not show complete self-preserving within the axial distance covered in the investigation. But for higher Reynolds numbers it tended to become self-preserving earlier for the same plate thickness in the wake. Drag co-efficient due to the wake was calculated from the momentum thickness equation (3.2.15) obtained by neglecting pressure gradient. Drag co-efficient was also calculated by applying equation (3.2.18) near the trailing edge of the plate, considering the effect of pressure gradient. The results obtained by the above two equations were in good agreement at each point with the experimental results obtained by Faruque [8]. The shape factor of the wake decreased with the increase of Reynolds number and with the axial distance from the trailing edge and it also decreased with decrease of plate thickness.

Toyoda and Shirahama [25] investigated experimentally the turbulent wakes subjected to presure gradients. The experiments were conducted in an open circuit wind tunnel for measuring mean velocity and turbulence characteristics.

The air delivered by an axial blower enter the test section through a nozzle via a settling chamber. The turbulence intensity ($\sqrt{u^2}/u_\infty$) at the exit of the nozzle was 0.003. A steel flat plate of 1.0 mm thickness and 1200 mm length was used as a wake generator. Mean velocities in boundary layers and wakes were determined from the measurements of total and static pressures. Turbulence intensities were measured with a constant temperature hot-wire anemometer. The results of the experiment were summarized as follows:

1) The total pressure along a streamline in the wake near the trailing edge with pressure gradient changed at approximately the same rate as with no pressure gradient along the same streamline.

2) The velocity defect distributions normalized with local scales and approach to the self-preserving solution downstream were not much affected by the pressure gradients.

3) The calculated results obtained by Toyoda and Hirayama [40] agreed well with the experimental data except for the strong pressure gradient.

2.3 Theoretical study

To find the form of the velocity profile in a two-dimensional wakes, Schlichting [15] used momentum equation of the form given by

$$uv + \frac{d}{dx}\int_{-\infty}^{\infty} u^2 dy + \ell^2 \left(\frac{du}{dy}\right)^2 = 0 \qquad (2.3.1)$$

in which the experession for turbulent shear stress was taken from Prandtl's old theory of turbulence ($\frac{\tau}{\rho} = \ell^2 \left|\frac{du}{dy}\right| \frac{du}{dy}$) and pressure gradient was neglected. The Prandtl's mixing length, ℓ was defined in terms of the width of flow,

$$\ell = cb \qquad (2.3.2)$$

The author defined the velocity profile in a conventional functional form $(u_\alpha - u) = (u - u_c)\, f(\eta)$, where $\eta = y/b$. To determine the velocity profile, Schlichting [15] used,

$$b = K_2 \sqrt{x} \qquad (2.3.3a)$$

and, $(u - u_c) = u_\alpha n / \sqrt{x}$ (2.3.3b)

Using the expression for ℓ and u_c in the momentum equation (2.3.1), an ordinary differential equation was derived in the following form

$$\eta f = \alpha_1 f'^2 \qquad (2.3.4a)$$

where, $\alpha_1 = 2c^2 n / k_2$ (2.3.4b)

Equation (2.3.4a) is subjected to the following boundary conditions:

1. At the edge of the wake ($\eta = y/b = 1$)

   $u_\alpha - u = 0$ and $\frac{d}{dy}(u_\alpha - u) = 0$, i.e. $f = f' = 0$ (2.3.5)

2. On the axis of the wake ($\eta = y/b = 0$)

   $u_\alpha - u = u_\alpha - u_c$, $\frac{d}{dy}(u_\alpha - u) = 0$, i.e. $f = 1$, $f' = 0$ (2.3.6)

The solution of the equation (2.3.4a) with boundary conditions given in equations (2.3.5) and (2.3.6) is,

$$(u_\alpha - u)/(u_\alpha - u_c) = f(\eta) = (1 - \eta^{3/2})^2 \qquad (2.3.7)$$

The constant, c, involved in the Prandtl's mixing length expression was determined to be 0.18, (f/b=0.18). The values of the constants k_2 and 'n' in the equations (2.3.3a) and (2.3.3b) can be determined by using Schlichting's [15] equations in the form, $n=1.4\sqrt{a_2}L$ and $k_2=0.8\sqrt{a_2}L$ where, a_2 is an empirical constant. For wake behind a two-dimensional cylinder, Schlichting [15] obtained experimentally the value of a_2 as 1.23.

To find the form of the velocity profile in an axisymmetric wake Taylor [10] used momentum equation of the form:

$$\frac{1}{y}\frac{d}{dx}\int_{\alpha}^{y}(u_\alpha - u)u_\alpha y\,dy + \ell^2\left(\frac{du}{dy}\right)^2 = 0 \qquad (2.3.8)$$

Here the expression for shear stress was taken in accordance with Prandtl's old theory. The Prandtl's mixing length, ℓ, was defined in terms of the width of the wake, $\ell = cb$. The author used the conventional functional form of the velocity profile given by

$$b = k\tfrac{3}{3}\sqrt[3]{x} \qquad (2.3.9a)$$

$$\text{and } u_\alpha - u_c = n_1 u_\alpha x^{-2/3}$$

After transformation he obtained for an axisymmetric wake, the same differential equation as for a two-dimensional wake:

$$\eta_f = \alpha_{2f}^2 f'^2 \qquad (2.3.10)$$

$$\text{where, } \alpha_2 = 3n_1 c^2. \qquad (2.3.11)$$

With the same boundary conditions given in equations (2.3.5) and (2.3.6), equation (2.3.10) may be integrated to give the same velocity profile as in a two-dimensional wake:

$$(u_\infty - u)/(u_\infty - u_c) = f(\eta) = (1-\eta^{3/2})^2 \qquad (2.3.12)$$

Reichardt [19] used momentum integral equation to find the form of the velocity profile in a two-dimensional wake. The author used Prandtl's new formula for shear stress given by:

$$\frac{\tau}{\rho} = \nu_t \frac{du}{dy}$$

where, $\nu_t = \chi\, b(u-u_c)$

If Prandtl's new formula for shear is used, the momentum equation for a two-dimensional wake takes the following form under constant pressure gradient:

$$2\frac{d}{dx}\int_{\infty}^{\delta} u_\infty(u_\infty - u)dy - \nu_t \frac{du}{dy} = 0 \qquad (2.3.13)$$

The velocity profile in the cross-section of a two-dimensional turbulent wake according to Prandtl's new theory of turbulance and Reichardt's theory [19] is

$$(u_\infty - u)/(u_\infty - u_c) = \exp(y^2/2\varepsilon_1 x) \qquad (2.3.14)$$

The constant ε_1 for a two-dimensional wake was determined from the experimental results of Schlichting [15] and Reichardt [19]

Reichardt [19] also obtained the following form of the velocity profile in an axially symmetric wake far from

the body:

$$(u_\infty - u)/(u_\infty - u_c)\ \exp(y^2/\ 2\overline{\varepsilon_1 x}^{2/3}) \qquad (2.3.15)$$

Hiroshi and Kuriki [14] also obtained the following form of the velocity profile for two-dimensional wakes behind flat plates

$$(u_\infty - u)/(u_\infty - u_c) = \exp(-a(y/y_{1/2})^2) \qquad (2.3.16)$$

where, $a = \ln 2$

Some solutions were obtained by using a computer program developed by Sinha, Fox and Winberger [26,27] for chemically non-reactive, quasi-parallel shear flows. The boundary layer equations with suitable boundary condtions were assumed to describe the motion of free shear flows. The governing equations were as follows:

Conservation of mass:

$$\frac{d}{dx}(\rho u y^2) + \frac{d}{dy}(\rho v y^j) = 0 \qquad (2.3.17)$$

Conservation of streamwise momentum:

$$\rho\left[u\frac{du}{dx} + v\frac{du}{dy}\right] = -\frac{dp_e}{dx} + 1/y^j \frac{d}{dy}\left(\mu y^j \frac{du}{dy}\right) \qquad (2.3.18)$$

where, j=0 and 1 for two-dimensional and axisymmetric flow, respectively. The associated boundary condition was

$$\frac{du}{dy} = 0$$

at the center line when y=0, for all values of x. The result was computed by using an implicit finite difference technique the details of which are described in refs. [26] and [27]. The results obtained were in close agreement with the available experimental data.

2.4 Recent Approach

The shear layers are recently investigated from the view point of its structure and eddy sizes. Such flow is identified to be irregular type with its structure in the coherent form. A coherent structure is a connected, large scale turbulent fluid mass with a phase-correlated vorticity over its spatial extent [28] . The presence of large-scale organized motions in the turbulent shear flows, apparent for a long time and implied by the mixing length hypothesis was suggested first by Townsend [29] and investigated in detail by Meller and others [30,31] . Near field coherent structure in wake was observed by flow visualization by the authors [32, 33] . A coherent structure is responsible for transports of significant mass, heat and momentum without necessarily being highly energetic itself. Sophisticated experimentation has been developed to investigate the coherent structure.

Differential methods of calculation is also an useful tool for predicting the turbulent flows in shear layers. The Turbulent model of semi-empirical equations developed by Launder, et.al [34] and others [35,36] are very powerful method for predicting flow.

CHAPTER - III

THEORY

3.1 General

Turbulent motion is governed by the continuity and the Navier-Stokes differential equations. Since the Navier-Stokes equations are non linear, exact analytical solutions to these equations have not yet been obtained. In order to apply Navier-Stokes equations to practical cases, hypothesis and empirical assumptions have to be introduced for obtaining a set of closed equations with time-averaged dependent variables. Here the conventional 'order of magnitude' principle is applied to the general momentum equation to obtain the equation in a simpler form. Later these equations are used for evaluating the wake properties.

Theoretical work on free shear flows can be developed in any of the following three classes of turbulent model: Class-1- turbulent viscosity models in which the length-scale of turbulence is found by way of algebraic formulae, Classs-2- turbulent viscosity models in which the length scale of turbulence is found from a partial differential transport equations, and Class-3-models in which the shear stress itself is the dependent variable of a partial differential conservation equation.

The Class-2 models have attracted the attention of the most of the researchers in this field. The models of Class-3 have not yet been refined sufficiently to achieve the level of universality of which they are belived to be capable. Therefore, engineering calculations of

turbulent flows have been confined to models of Class-1 and Class-2.

3.2. Governing Equations

Assuming steady, incompressible flow, constant fluid properties, boundary layer approximations and applying the 'order of magnitude' principle, the mass and momentum conservation equations in two-dimensional flow can be written in the following form:

$$\frac{du}{dx} + \frac{dv}{dy} = 0 \qquad (3.2.1)$$

$$u \frac{du}{dx} + v \frac{du}{dy} = \frac{1}{\rho} \frac{d\tau}{dy} \qquad (3.2.2)$$

where, τ is the shear stress and ρ is the density of the fluid. The flow configuration and co-ordinate system are shown in fig. 3.1. The shear stress includes both viscous and turbulent contributions and it is written as

$$\frac{\tau}{\rho} = \nu \frac{du}{dy} - \overline{u'v'} \qquad (3.2.3)$$

where, ν is the molecular diffusivity. The turbulent part of shear stress is $-\rho \overline{u'v'}$ and it is expressed by Boussinesq's hypothesis:

$$-\rho \overline{u'v'} = \rho \nu_T \frac{du}{dy} \qquad (3.2.4)$$

where, ν_T is the turbulent diffusivity. For the turbulent wake, the diffusivity, ν_T is expressed in terms of Prandtl's mixing length, ℓ and mean velocity gradient, $\frac{du}{dy}$

$$\text{i.e. } \nu_T = \ell^2 \frac{du}{dy} \qquad (3.2.5)$$

where, ℓ is Prandtl's mixing length. According to Prandtl's velocity distribution principle the relation between mixing length and vertical distance, y is

$$\ell = \chi y; \quad \chi = 0.4 \tag{3.2.6}$$

Where, χ = dimensionless empirical constant. Which must be obtained from experiments. Hence, according to Prandtl's assumption, by neglecting molecular diffusivity term the turbulent shear stress becomes.

$$\tau_t = \chi^2 \rho y^2 \left(\frac{du}{dy} \right)^2 \tag{3.2.7}$$

So the final differential form of momentum equation for turbulent wake is

$$u \frac{du}{dx} + v \frac{du}{dy} = 2\chi^2 \left[y \left(\frac{du}{dy} \right)^2 + y^2 \left(\frac{du}{dy} \right) \left(\frac{d^2u}{dy^2} \right) \right] \tag{3.2.8}$$

where, all variables are dimensionless quantities.

By using the von Kármán shear stress equation(D.10) (which is discussed in Appendix-D), the momentum equation can be expressed as

$$u \frac{du}{dx} + v \frac{du}{dy} = \chi^2 \left[4 \left(\frac{du}{dy} \right)^3 \left(\frac{d^2u}{dy^2} \right)^2 - 2 \left(\frac{du}{dy} \right)^4 \left(\frac{d^3u}{dy^3} \right) \right] \Big/ \left(\frac{d^2u}{dy^2} \right) \tag{3.2.10}$$

Again applying the order of magnitude principle and using equation (3.2.1), the momentum equation may be written

as [37]

$$\frac{d}{dx}\bar{u}(u-u_\infty)+\frac{d}{dy}v(u-u_\infty)+\frac{d}{dy}\overline{u'v'}=0 \qquad (3.2.9)$$

The pressure gradient and the effect of molecular viscosity are neglected in the above equation. In wake, $u-u_\infty$ vanishes at sufficiently large values of y, and it does so for $\overline{u'v'}$. Integrating equation (3.2.9) with respect to y over the entire flow, we obtain

$$\frac{d}{dx}\int_{-\infty}^{\infty}u(u-u_\infty)\,dy=0 \qquad (3.2.10)$$

The total momentum defect in a wake is constant,

so, $$\rho\int_{-\infty}^{\infty}u(u-u_\infty)dy=M \qquad (3.2.11)$$

The momentum integral equation (3.2.11) can be used to define a length scale for turbulent wakes. Imagining that the flow past an obstacle produces a completely separated, stagnant region of width 2θ, $2\rho u_\infty^2\theta$ represents the net momentum defect per unit time and depth.

Thus, $$-2\rho u_\infty^2\,\theta=M \qquad (3.2.12)$$

Equating equation (3.2.11) and (3.2.12),

$$-2\rho u_\infty^2\theta=\rho\int_{-\infty}^{\infty}u(u-u_\infty)\,dy$$

or, $$\theta=\int_0^{\infty}\frac{u}{u_\infty}(1-u/u_\infty)dy \qquad (3.2.13)$$

where, θ is called the momentum thickness of the wake. The momentum thickness is related to the drag co-efficient of the obstacle that produces the wake. The drag co-efficient, Cdm, is defined by,

$$D_1=-\tfrac{1}{2}\,Cdm\,\rho\,u^2L \qquad (3.2.14)$$

where, D_1 is the drag per unit depth and L is the

characteristic height of the obstacle. The drag, D_1, produced the momentum flux, M. So, equating equations (3.2.12) and (3.2.14.),

$$2\rho u_\alpha^2 \theta = \tfrac{1}{2} Cdm \; u_\alpha^2 L$$

or $$Cdm = 4\theta/4 \qquad (3.2.15)$$

The momentum integral equation for drag on the obstacle having pressure gradient is given by

$$D_1 = L\left[\int_{-\alpha}^{\alpha}(P_o + \rho u_o^2)\,dy - \int_{-\alpha}^{\alpha}(p + \rho u^2)dy\right] \qquad (3.2.16)$$

But according to the definition of drag coefficient

$$D_1 = \tfrac{1}{2} Cd\; u_o^2 L \qquad (3.2.17)$$

Equating equations (3.2.16) and (3.2.17), we have,

$$\tfrac{1}{2} Cd\,\rho u_o^2 L = L\left[\int_{-\alpha}^{\alpha}(p+u_o^2\rho)dy - \int_{-\alpha}^{\alpha}(p+\rho u^2)dy\right]$$

or, $$Cd = \frac{1}{1/2}\rho u_o^2 \int_{-\alpha}^{\alpha}(p_o - p)dy + 2\int_{-\alpha}^{\alpha}(1-u^2/u_o^2)dy \qquad (3.2.18)$$

The displacement thickness, δ^* is that distance by which external potential field of flow is displaced outwards as a consequence of the decrease in velocity in the boundary layer. The decrease in volume flow due to the influence of friction is

$$\int_{\substack{y=o\\ y=o}}^{\alpha}(u_\alpha - u)dy$$

so that

$$u_\alpha \delta^* = \int_{y=o}^{\alpha}(u_\alpha - u)dy$$

or, $$\delta^* = \int_{y=o}^{\alpha}(1-u/u_\alpha)dy \qquad (3.2.19)$$

3.3 Initial Condition

The initial velocity distribution for wake is given by the semi - empirical equation

$$u/u_\infty = (y/\delta)^{\frac{1}{n}} \qquad (3.3.1)$$

where, δ is the initial boundary layer thickness, which is found from experimental results and 'n' is the power index which is found from limiting case of the equation (3.2.13). Calculation of 'n' is shown in the Appendix-C.

3.4. Boundary Conditions

Basic differential equations(3.2.1) and (3.2.9) and other empirical equations governing the mean flow were solved numerically. The appropriate boundary conditions applicable to equations (3.2.1) and (3.2.9) are:

$$-\frac{du}{dy}(x,1)=0,\ v(x,1)=0,\ u(x,\delta)=u_\infty \qquad (3.4.1)$$

3.5 Self-Preservation Equation

The mean velocity distribution for self-preserving wake is given by the following semi-empirical equation

$$(u_\infty - u)/(u_\infty - u_c) = \exp\left(-a(y/y_{1/2})^2\right) \qquad (3.5.1)$$

where, $a = \ln 2$

A semi-empirical relation for half width of the wake follows from the measurements of Schlichting and Reichardt [19]

$$y_{1/2} = 0.35\sqrt{x}\sqrt{C_d m L} \qquad (3.5.2)$$

3.6 Solution of the Equations

An explicit finite difference scheme was used to solve the conservation and other equations.

3.7. Calculation Technique

The method of approximating the derivatives is given in Appendix-B. The finite difference grid used for the calculation is shown in Fig.3.1. The computer program developed for this purpose has the capability of handling non-uniform grid spacings in both x- and y- directions. For calculating mean flow properties from continuity and momentum equations, non-uniform grid spacings were used in X -direction which were restricted by the stability conditions. At starting, first level information is obtained from initial conditions and second level information is obtained from the finite difference solutions. This scheme requires only the previous step values.

The other flow characteristics were calculated by using the different empirical relations and mean flow properties found from continuity and momentum equations.

CHAPTER - IV

RESULTS AND DISCUSSION

4.1 General

Empirical formulae and experimental values of flow parameters at the trailing edge were used for calculating the flow properties in the wake at the downstream of the trailing edge. The differential mass and momentum equations were solved by using boundary conditions given in Art.3.4. The investigation was carried out for four Reynolds numbers, $Re\theta e=2.18x10^3$, $2.01x10^3$, $2.01x10^3$, $1.9x10^3$ and $1.7x10^3$. For all the four cases, the same computer program was used with different values of the parameters involved. The computer program is given in Appendix-E. The computational analysis were performed by using the IBM-4331 computer of the BUET Computer Center.

This chapter presents discussions on the results obtained by the present study and comparisons of these results with the experimental measurements of Faruque [8] and other predicted results.

4.2 Trailing Edge Conditions

From the trailing edge the wake originates and spreads downstream. The character of the wake depends upon the trailing edge conditions. Near the trailing edge the velocity increases in the transverse direction and follows

the boundary layer velocity profile. As the boundary layer is thin, the velocity gradient in the transverse direction is high. Fig.4.1 shows velocity distributions for the Reynolds numbers 2.18×10^3, 2.01×10^3, 1.9×10^3 and 1.7×10^3 the experimental data being taken from Faruque [8]. The Reynolds number was defined on the basis of momentum thickness and free-stream average velocity. The experimental values of the mean velocities shown in Fig. 4.1 were fitted to the empirical equation (3.3.1). It is observed from Fig.4.1 that the empirical equation (3.3.1) fits closely with existing experimental results. The rms deviation did not exceed 0.11257 for any case. The experimental values of the mean velocity at the trailing edge were also plotted in the universal coordinate system in Fig.4.2. The nature of the curves in Fig. 4.2 implies that the flow over the trailing edge was fully develped turbulent flow. Islam [1] has identified that the initial conditions have a significant influence on the development of shear layer of jets. As the development of wake is similar to that of jet flows, it is likely that the initial conditions will influence the wake flows. The characteristics of the turbulent boundary layer at the trailing edge of the plate for different flow parameters are shown in Table-4.1

TABLE -4.1

CHARACTERISTICS OF THE VELOCITY PROFILE
AT THE TRAILING EDGE OF THE PLATE (Ref.8)

Average free-stream velocity U_{av}(m/sec.)	Momentum thickness θ (cm)	Reynolds Number $Re_{\theta e}$	Boundary Layer thickness δ (cm)	Friction velocity u* (m/sec)
18.10	0.0894	2.18×10^3	0.762	0.832
13.49	0.1107	2.01×10^3	0.985	0.683
9.99	0.1422	1.9×10^3	1.39	0.509
7.65	0.1651	1.7×10^3	1.6	0.418

4.3 Shear Stress model

Different shear stress models given by equations(D.4), (D.6) and (D.10) were applied to the equations governing the flow to express the turbulent shear stress. It is seen that the Boussinesq eq.(D.4) model is suitable for only fully developed turbulent flow at the trailing edge. The von Kármán eq.(D.10) model is suitable where mixing length is dependent on space Co-ordinates but it does not seem suitable for present turbulent wake for both developing and developped regions. With the Prandtl's model, eq.(D.6) the results obtained by finite difference method were in close agreement with the experimental results of Faruque [8].

4.4 Free-Stream Flow.

The free-stream velocity, u_∞, represents the uniform flat part of the velocity profile outside the shear or boundary layer and it is parallel to the x-axis. The free-stream velocity in the wake drops instantaneously when the boundary layer separates from the plate. Such drop is observed up to the axial distance $x/\theta=55$,(Fig.4.3), after which it achieves a constant value. From the consideration of potential flow theory, there exists adverse axial pressure gradient at the beginning of the wake and it achieves zero axial pressure gradient after $x/\theta=55$. The drop of the uniform free-stream velocity is due to the increase of flow area as the profile separates from the plate. The finite difference results are similar to those given in Fig.4.3. The calculated results of free-stream velocity for different Reynolds number are in close agreement with the existing experimental results shown in Fig.4.3. The rms value for deviation of the theoretical and experimental results are found within the range of 0.0 to 0.03194.

4.5. Wake Development

4.5.1 Velocity and Shape Factor

Fig.4.4a, 4.4b, 4.4c and 4.4d show the variations of mean velocity distribution in wake for Re $\theta e=2.18\times10^3$, 2.01×10^3, 1.9×10^3 and 1.7×10^3 respectively. Because of high velocity gradient, the wake near the plate is likely to be complicated. The vortex form from the surface of the plate is being convected into the flow direction and

diffused by viscosity. It follows that convection is ultimately more important that the streamwise diffusion and that streamwise velocity gradient is small compared with that in the lateral direction at the downstream. As the velocity gradient gradually decreases with the axial distance, the flow tends to become self-preserving with the increase of axial distance. Fig., 4.4a, 4.4b, 4.4c and 4.4d show the development of the wake with increasing width. Such a spread of the wake is logical from the view point of energy transfer to the wake from the surroundings. The velocity distribution curves near the plate shows better agreement with the existing experimental results than that at the far distance from the plate. The rms deviation is within the range from 0.0012 to 0.0321.

The momentum thickness within the wake was calculated by using equation(3.2.13) at different axial distances in the downstream of the wake. The values of momentum thickness for diffrent Re θe are shown in Fig.4.5. The wake momentum thickness increases with increase of Re θe.

The shape factor, $H=\delta^*/\theta$, is plotted in Fig.4.6 as a function of axial distance and compared with the results of Faruque[8]. The slope of the curve for any Reynolds number decreases at a higher rate in the region close to the trailing edge and at a slower rate with the

increase of axial distance. This trend of the shape factor curves in Fig.4.6 shows an indication of self-preservation of flow. The flow will be absolutely self-preserving when the shape factor tends to be unity. The shape factor varies with Reynolds number, Re θe, as shown in Fig.4.6. The results presented in Fig.4.6 are in satisfactory agreement with the experimental results of Faruque [8] . The rms deviation of the present results with the experimental results is found within the range from 0.002 to 0.066.

4.5.2 Half Width and Center-line Velocity

The half width is an important geometrical dimension for length scale, generally used for explaining the self-preserving characteristics of a flow. Dimensionless half width ($\frac{4}{3} y_{\frac{1}{2}} / CdmL$) of the wake is plotted against axial distance in Fig.4.7. Half width of the wake which is calculated from the semi-empirical equation(3.5.2) given by Schlichting [15] for two-dimensional wakes are plotted in Fig.4.7. It is seen that the axial variation of the present calculated half width of the wake near the trailing edge of the plate deviates from that of existing experimental results, but it agrees with empirical results from the trailing edge. Fig.4.7 also presents the fact that with the decrease of the initial boundary layer thickness for higher Reynolds number, the existing experimental results approach towards present theoretical results. It is also to be noted that the effect of the initial conditions exists only upto a certain axial

distance and then the flow becomes independent of the state of origin. Similar case is also explained by Islam [1] and Hussain and Zedon [38] for jets. This is also probably due to the nature of energy transfer from large scale to small scale eddies which depends on vortex pairing.

The spread parameter for the wake is shown in Fig.4.8 which achieves approximately a constant value of δ=0.675 at x/D=125 for the Reynolds numbers studied. Near the trailing edge of the plate the spread parameter decreases rapidly upto x/D=125. The present results are in close agreement with existing experimental results of Faruque [8].

Dimensionless center-line velocity defect is plotted in Fig.4.9 against the dimensionless axial distance, x/CdmL. For the four different Reynolds numbers, the calculated values of center-line velocity defect falls on the same line except for Re $\theta e=2.18\times10^3$. Velocity defect decreases sharply at the trailing edge due to high velocity gradient, but decreases slowly at axial distance far away from the plate. The plot in Fig.4.9 also shows a comparison with the experimental results of Faruque [8] and Schlichting [15]. Near the trailing edge velocity defect is same as that of Faruque's [8] experimental results. But after x/CdmL $>$ 40, the present velocity defect is less than that of Faruque's[8] experimental results, though it comes closer to the Schlichting's [15] values.

4.5.3 Self-Preservation

Dimensionless velocity distribution for the wakes

are shown in Fig.4.10a, 4.10b, 4.10c and 4.10d corresponding to the Reynolds numbers Re θe, 2.18×10^3, 2.01×10^3, 1.9×10^3 and 1.7×10^3 to examine their self-preservation. The half width, $y_{1/2}$ is used as length scale in the self-preservation plot. The velocity distribution in Fig.4.10a, 4.10b, 4.10c and 4.10d do not show self-preservation, because they become similar only at large distances downstream from the trailing edge. No similarity of mean velocity profile is observed near the trailing edge of the plate. The experimental results of Faruque [8] for similarity profile are also shown in Fig.4.10a, 4.10b, 4.10c and 4.10d for comparison. It is seen that after certain axial distance, x/D=16, the present results fall on the same line. Deviation of the existing experimental results of Faruque [8] from the present computational results may be expressed as rms deviation. This rms deviation was found to decrease gradually with the axial distance as shown in Table 4.2. The least rms deviation is an indication of self-preservation. Examining the rms deviation in Table 4.2, it can be concluded that flow achieves self-preservation earlier in the flow with the higher Reynolds number, Re θe. From a comparison of Fig.4.10a and Fig.4.10d, it is clear that the flow is nearer to self-preservation in Fig.4.10a for Re $\theta e = 2.18 \times 10^3$ than that in Fig.4.10d for Re $\theta e = 1.7 \times 10^3$ at x/D=48. The values of rms deviation for various Reynolds number, Re θe are plotted in Fig.4.11 to show that the rms deviation is less for higher Reynolds number at any axial distance.

So the wake velocity profile becomes self-preserving earlier for higher Reynods number.

Drag Co-efficient due to the wake was calculated from the momentum thickness equation(3.2.15) obtained by neglecting pressure gradient. The drag Co-efficient was plotted in Fig.4.12 which shows that it increases with the Reynolds number.

TABLE - 4.2

rms DEVIATIONS AT VARIOUS DISTANCES FROM THE TRAILING EDGE OF THE PLATE

x/D / Re θe	16	24	48
2.18×10^3	0.066	0.062	0.06
2.01×10^3	0.072	0.069	0.0675
1.90×10^3	0.078	0.076	0.075
1.70×10^3	0.095	0.0935	0.0925

CHAPTER - V

CONCLUSION

The present investigation is on the two-dimensional tubulent wakes formed behind a flat plate. A computer program has been developed to solve the equations of mass and momentum conservation using explict finite difference scheme.

Numerical calculations were performed for mean velocity, half width and other flow geometry and characterstics in the wake region for four different exit Reynolds numbers, i.e. Re $\theta e = 2.18 \times 10^3$, 2.0×10^3, 1.9×10^3 and 1.7×10^3. The boundary layers were turbulent at the trailing edge of the plate, and the wake formed with these boundary layers were assumed to be turbulent at the exit. The initial boundary layer was identified to be turbulent on the basis of the experimental values of velocities.

The results obtained by present calculation were compared with existing experimental measurements. The agreement of the present results of most of the parameters with experimental results of Faruque [8] indicates that Prandtl's mixing length model is satisfactory to expresses the turbulent shear stress in the wake. The momentum thickness increases with the increase of Reynolds number. The shape factor of the wake decreases with the increase of Reynolds number and with the axial distance from the trailing edge. The decrease of the shape factor to unity is an indication of self-preservation of flow. The velocity distribution in the neighbourhood of the flat plate is

unstable due to the presence of high velocity gradient in the axial direction and it decreases gradually to become self-preserving. The axial variation of half width of the wake is approximately linear except close to the trailing edge. The present results agree with the existing experimental results after an axial distance x/CdmL=50, where the effect of initial conditions are insignificant. The rate of increase of the center-line velocity is rapid in the near region of the wake and it becomes slow with the increase of axial distance. The flow within the wake does not show complete self-preserving within axial distance covered in the investigation. But at higher Reynolds number it tends to become self-preserving earlier for the same plate thickness at the beginning.

REFERENCES

1. Islam, S.M.N., "Prediction and Measurement of Turbulence in the Developing Region of Axisymmetric Isothermal Free Jets", Ph.D. Thesis, Deptt. of Mech. Engg., University of Windsor, Windsor, OWT, Canada, 1979.

2. Madni,I and Pletcher, R.H., "Prediction of Turbulent Jets in Coflowing and Quiescent Ambients", ASME Journal of Fluid Engineering, Vol.97, Dec.1975,PP. 558-567.

3. Boussinesq, J., "Essaisur La Theoric des Eaux Courantes", Mem Press. Acad. Sci. xxiii, 46, Paris (1877)

4. Prandtl,L., "Bericht Uber Untersuchungen Zur Ausgebildeten Turbulenz", ZAMM, Vol.5, 1925, PP.136.

5. Von Karmán,T., "Mechanische Ahnlichkeit und Turbulenz", Nachr. Ges.Wiss.Gottingen, Math. Phys. Klasse, 58(1830)

6. Bradshaw P.,Ferriss, D.H., and Atwell, N.P.,"Calculation of boundary-layer development using the turbulent energy equation", JFM 28, P.593-616(1967)

7. Habib and Whitelaw., "Velocity Characteristics of Confined Co-axial Jet", ASME Transaction, Vol.101, Dec. 1979.

8. Faruque,P.K.O.,"Experimental Investigation of Two-Dimensional Wakes Behind Flat Plates", M.Sc.Engg.(LE). Thesis. Deptt. of Mech.Engg., B.U.E.T., Dhaka, November, 1983.

9. Prandtl, L., "Bemerkungen Zur Theorie der Freien Turbulenz", ZAMM 22, P.241-243(1942) Also Coll.Works II, P. 869-873.

10. Taylor.G.I, "The Transport of Voticity and Heat Through Fluids in Turbulent Motion", Appendix by A. Fage and V.M. Faulkner. Proc.Roy.Soc.London A 135,P.685-705(1932)

11. Keffer,J.F., "The Uniform Distribution of a Turbulent Wake", J.F.M., Vol.22, part-1, 1965, P.135.

12. Keffer, J.F., "A Note on the Expansion of Turbulent Wakes", JFM., Vol.28, Part-1, 1966, P.183.

13. Chevray,R. Kovasznay, L.S.C.,"Turbulence Measurements in the Wake of a Thin Flat Plate", AIAA Journal, Vol.7, No. 8, August, 1969, P.1641.

14. Hiroshi,S. and Kuriki, K., "The Mechanism of Transition in the Wake of a Thin Flat Plate Placed Parallel to a Uniform Flow", JFM., vol.11,1961, P.321.

15. Schlichting, H.,"Uberrdass Ebene Winds Chatten Problem", Thesis Gottingen, Ingr. Arch. 5, 1930, P.533.

16. Hall,A.A. and hislop,G.S., "Velocity and Temperature distribution in the Turbulent Wake Behind a Heated Body of Revolution ", Prac. Cambridge Phi.Soc.34,1938, P.345.

17. Gartshore, I.S., "Two Dimensional Turbulent Wake", JFM., vol.30, Part-3, 1930, P.533.

18. Swain, L.M.,"On the Turbulent Wake Behind a bdoy of Revolution" Proc. Roy. Soc. (London), A, 135, 799, 1929, P.647.

19. Reichardt,H.,"Gesetzmassigkeiten der Freien Turbulenz", VDI-Forschungsh,1951, P.414.

20. Goldstein, S., "Note on the Velocity and Temperature Distribution in the Turbulent Wake Behind a Heated body of Revolution", Proc. Cambridge Phill.Soc.34, 1938, P.351.

21. Demetriades, A., "Mean Flow Measurements in an Axisymmetic Compressible Turbulent Wakes", AIAA Journal, vol.6, No.3, 1968, p.482.

22. Fage, A. and Falkner, V.M.,"The Transport of Vorticity and Heat Through Fluids in Turbulent Motion", Proc.Roy.Soc. (London), A,135, Appendix,1932.

23. Islam,S.M.N.,"Design and Construction of Closed Circuit Wind Tunnel", M.Sc.Engg. Thesis, Deptt. of Mech. Engg. BUET, Dhaka, 1975.

24. Khalil, G.M.,"The Initial Region of Plane Turbulent Mixing Layer", Ph.D. Thesis, Deptt. of Mech. Engg. B.U.E.T., Dhaka, 1982.

25. Toyoda,K and Shirahama Y,"Turbulent Near Wakes in Presure Gradient", Hokkaido Institute of Technology, Sappora, Japan. Vol. A.8-13 Dec. 1980. First Asian Congress of Fluid Mechanics.

26. Sinha, R. Fox, H. and Weinberger,L., "An Implicit Finite Difference Solution for Jet and Wake Problems", Pt.I. Analysis and Test cases. ARL 70-0025, U.S. Air Force, Feb. 1970.

27. Sinha, R.,Fox, H. and Weinberger, L., "An Implicit Finite Difference Solution for Jet and Wake Problems", Pt.II; Program Manual. ARL 70-0024, U.S. Air Force, Feb. 1970.

28. Hussian, A.K.M.F., "Coherent Structures", Aerodynamics and Turbulence Laboratory, July, 1921, .6.

29. Townsend, A.A., "The Structure of Turbulent Shear Flow", Cambridge U. Press(1956).

30. Meller, G.L. and Hering, B.J., "Two Methods of Calculating Turbulent Boundary Layer Behavior Based on Numberical Solution of the Equation of Motion", D.J. Cockrell, eds Stanford University C.1969, p.331.

31. Payne, F.R. and Lumley, J.L., Phys Fluid Suppl., 10,5194(1967)

32. Brown, G.B., Physical Sec.47, 1935, P.703.

33. Anderson, A.B.C., J., Acous.Sec.Amer, 26,1954, P.21.

34. Launder, B.E., Morse, A., Rodi, W. and Spalding, B.B., "A Comparison of the Performance of Six Turbulent models", Proc. Hypersonic Aircraft Fluid Mechanics Branch, NASA Langley Research Center, Mapton, Firgine, 1924-1972.

35. Korst, H.H. and Chow, W.L., "On the Correlation of Analytical and Experimental Fresh Shear Layer Similarity Profiles by Spread Rate Parameters", Trans. ASME, ser D.J. Basic Engg., Vol.93, No.3, Sept. 1971, P.377.

36. Schetz, J.A., "Some Studies of the Turbulent Wake Problem", Astronant. Acta, Vol.16, No.2 Feb.1971, P.107.

37. Abramovich, G.N.,"The Theory of Turbulent Jets", The M.I.T., Press, Massachusetts Institute of Technology, Cambridge, Massachusetts.

38. Hussain, A.K.M.F and Zedan, M.E., "Effect of the Initial Condition on the Axisymmetric Free Shear Layer", Physics of Fluid, Vol.24, No. 9, Sept, 1978, P.1475.

39. Azim., M.A., "Numerical Computation for Velocity and Temperature Within the Axisymmetric Turbulent Jets in Moving Surroundings", M.Sc.Engg.(ME) Thesis. Deptt. of Mech.Engg.BUET, Dhaka,1985.

40. Toyoda and Hirayama(1975)"Turbulent Near Wake of a Flat Plate", (Part-2)Bull,JSME,Vol.18,No.120 PP.605-611.

F I G U R E S

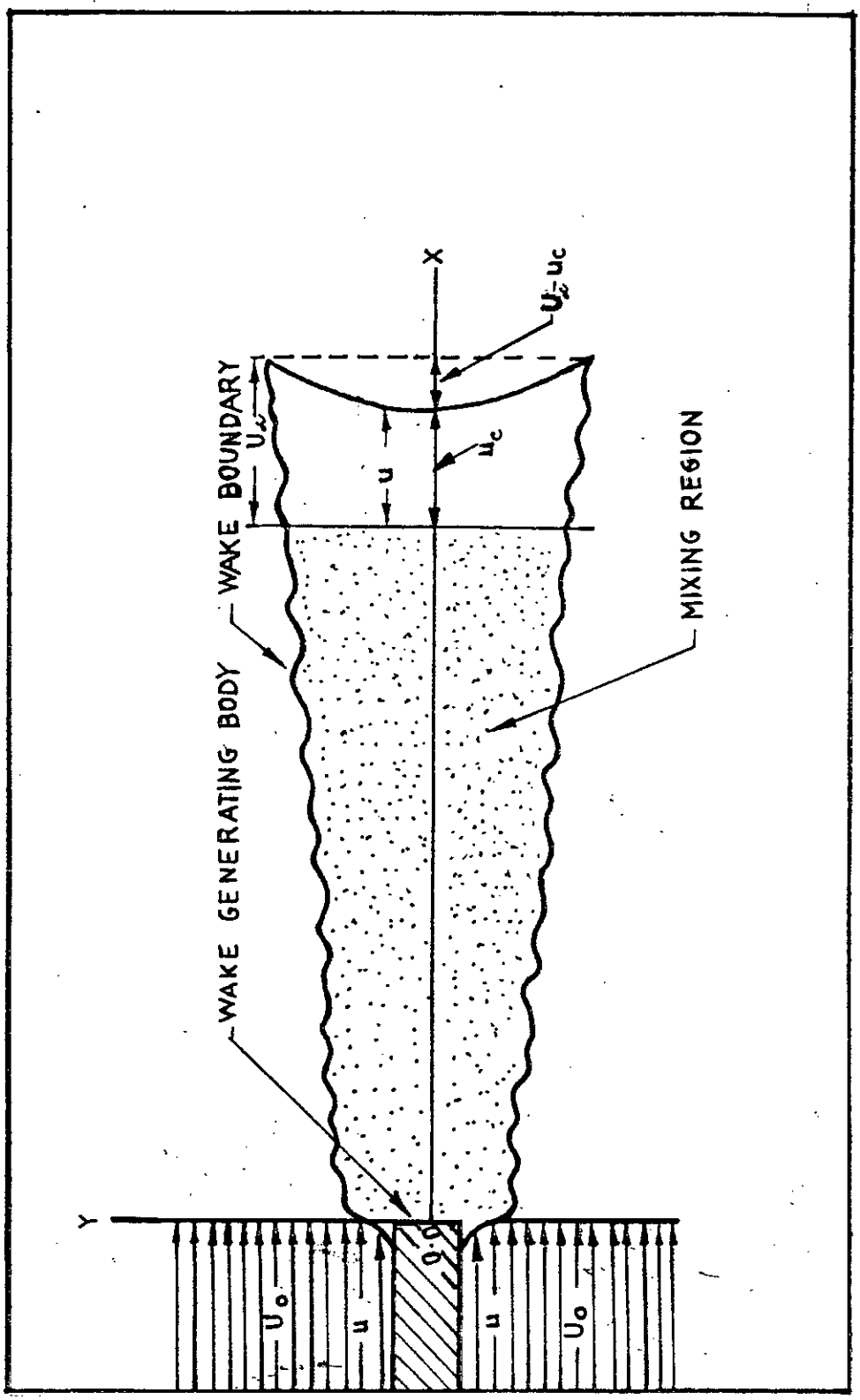

FIG.1.1 WAKE GEOMETRY AND NOMENCLATURE

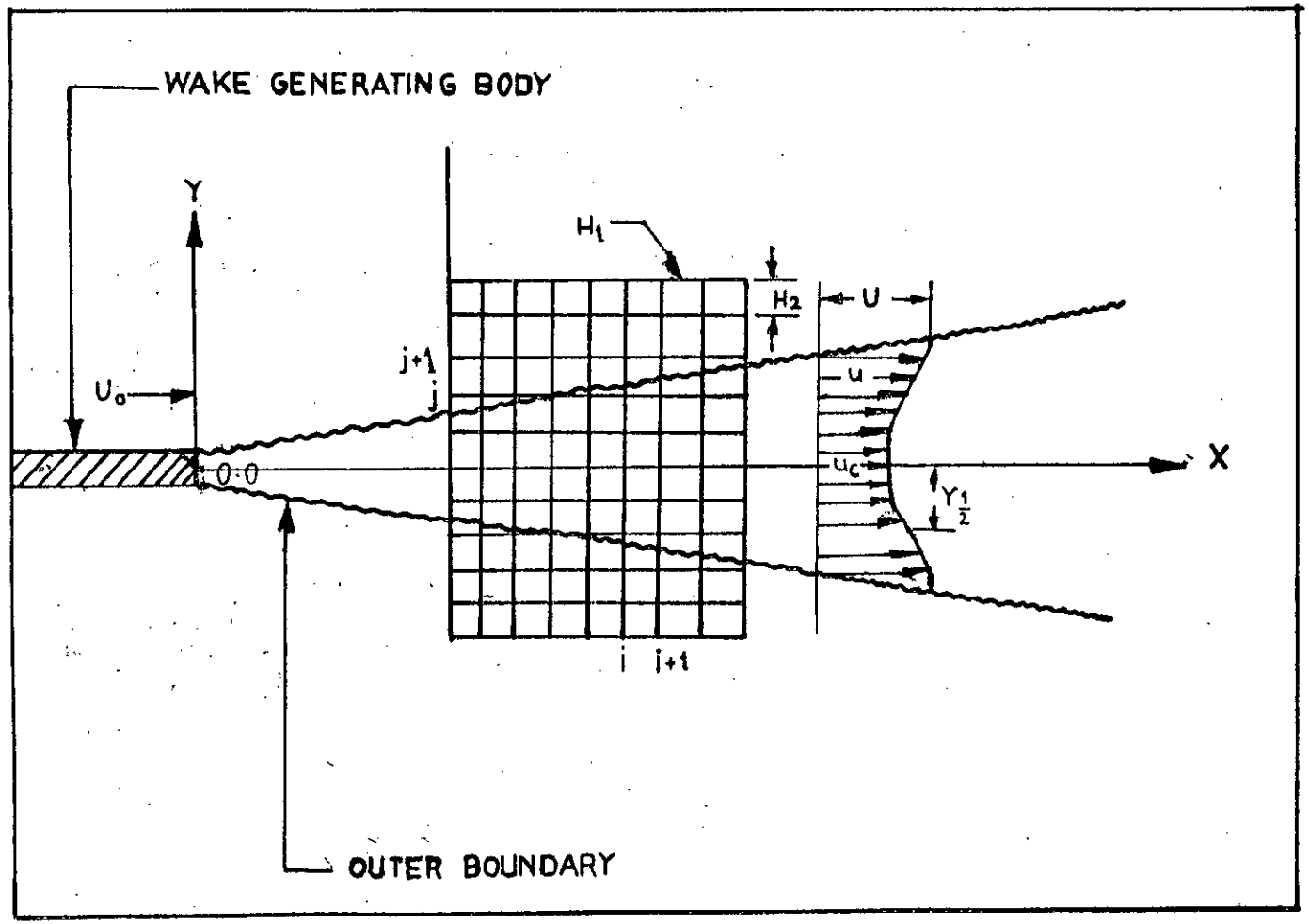

FIG. 3·1 CO-ORDINATE SYSTEM OF WAKE
AND
FINITE-DIFFERENCE GRIDS

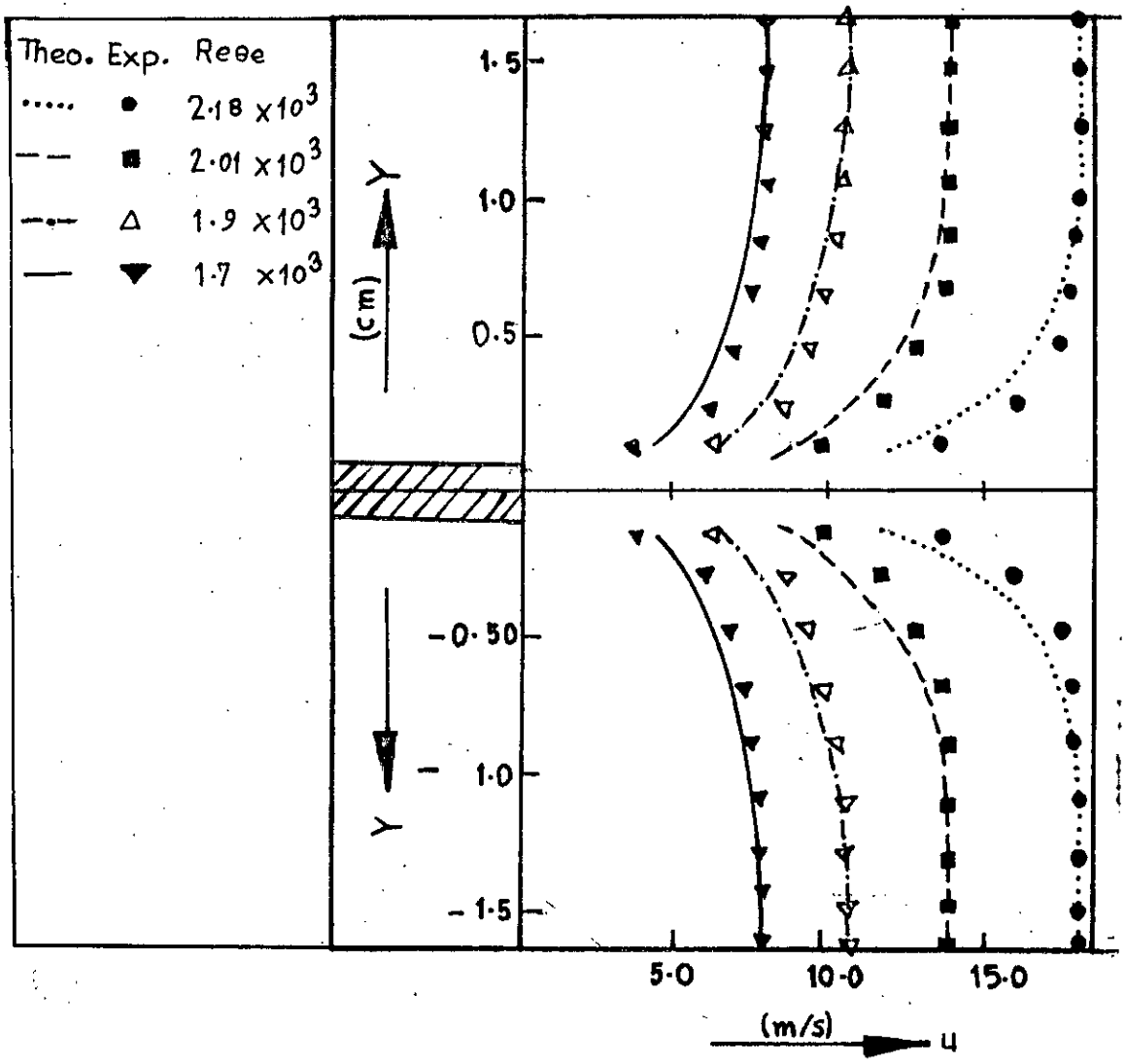

FIG. 4·1 MAGNIFIED TRAILING EDGE VELOCITY PRI
PROFILE

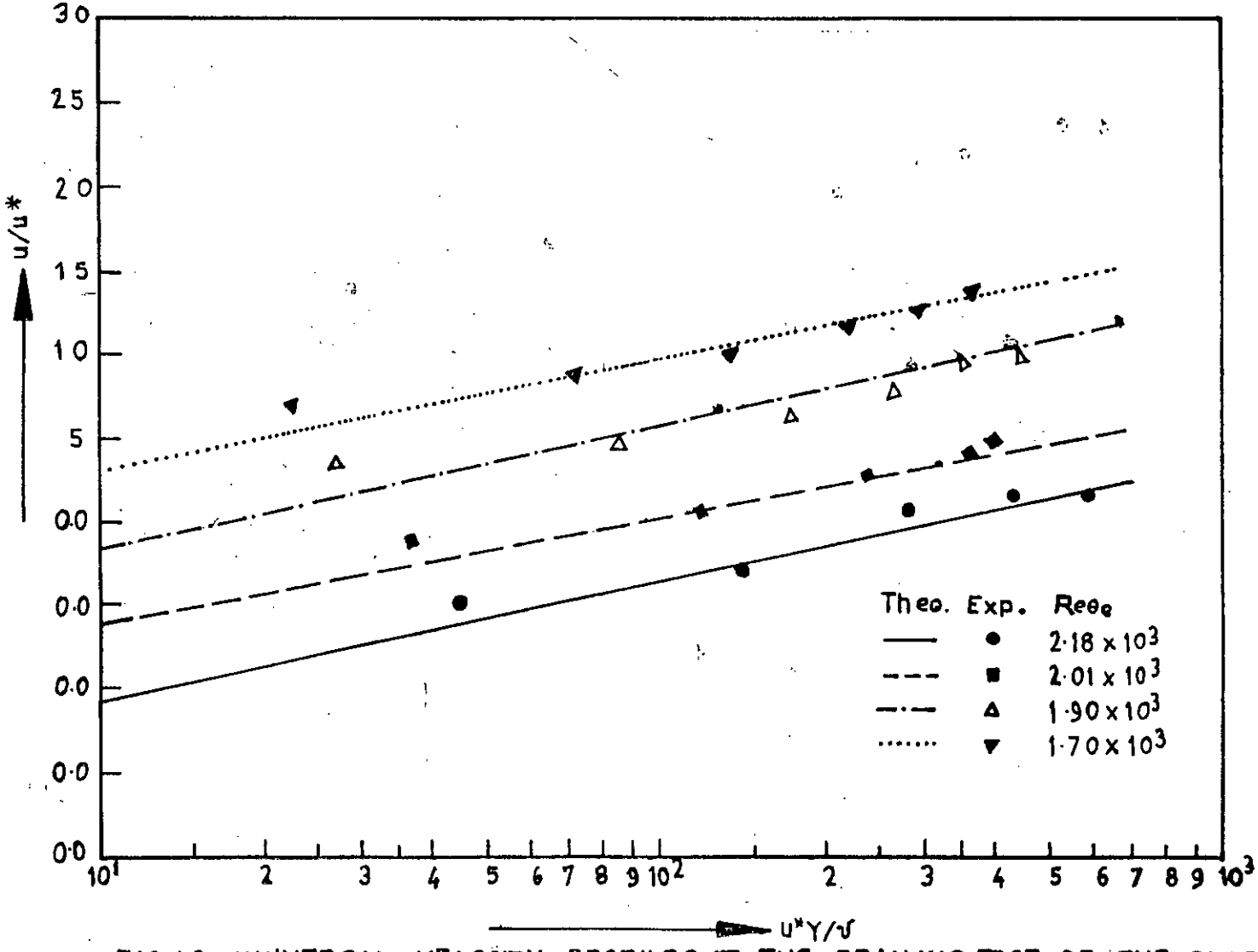

FIG.4.2 UNIVERSAL VELOCITY PROFILES AT THE TRAILING EDGE OF THE PLATE

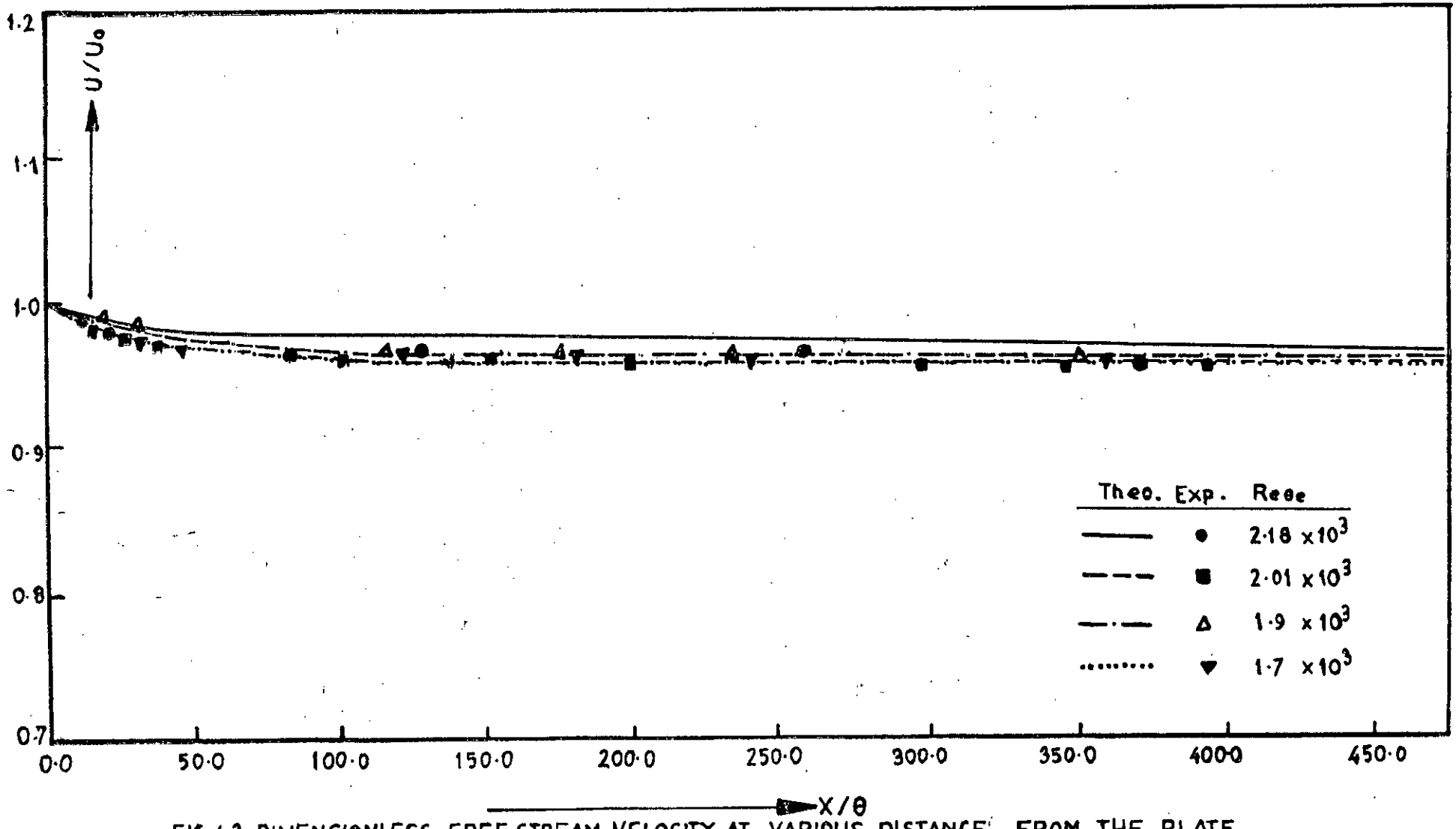

FIG.4.3 DIMENSIONLESS FREE-STREAM VELOCITY AT VARIOUS DISTANCE FROM THE PLATE

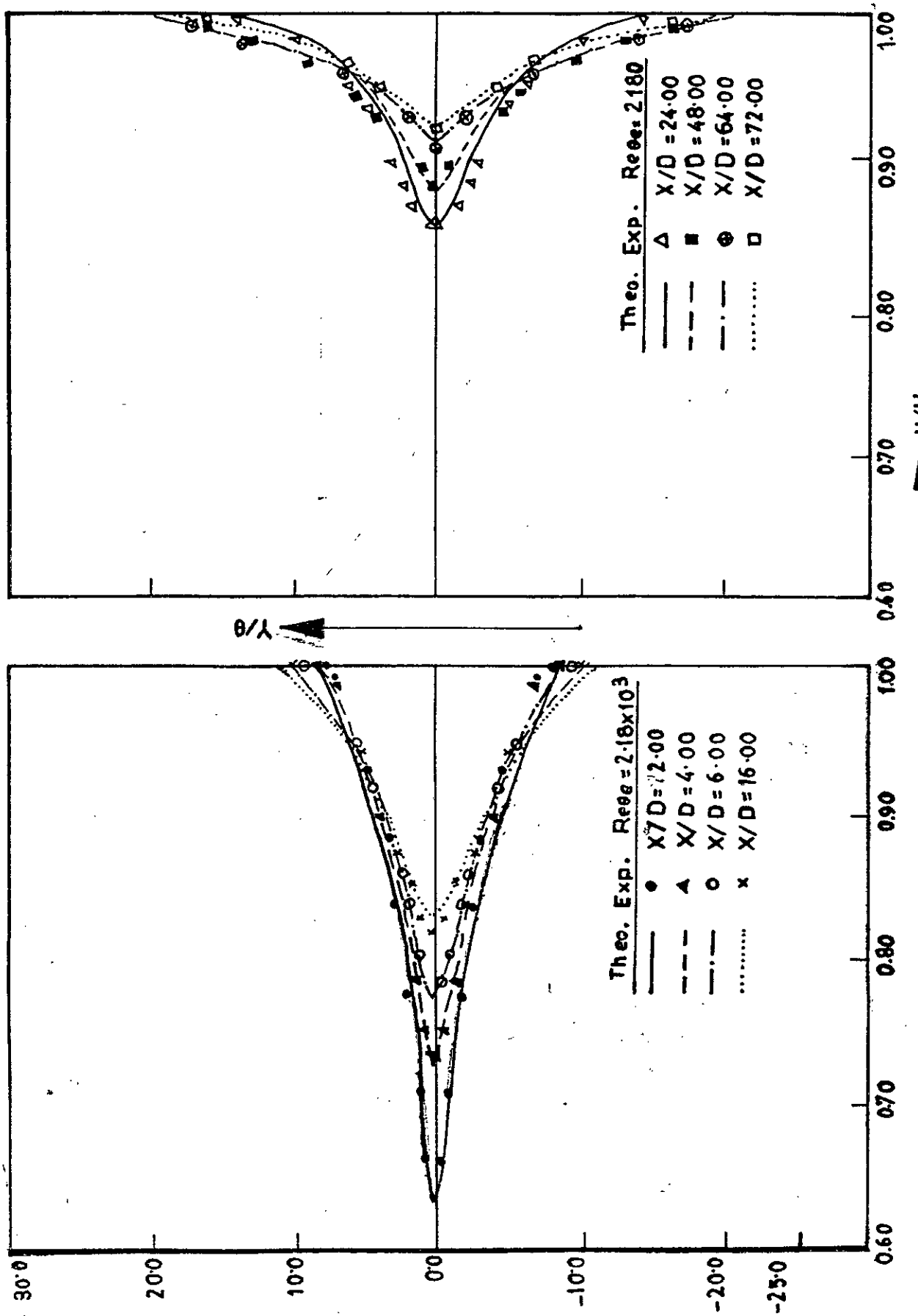

FIG. 4.4a MEAN VELOCITY DISTRIBUTION IN WAKE

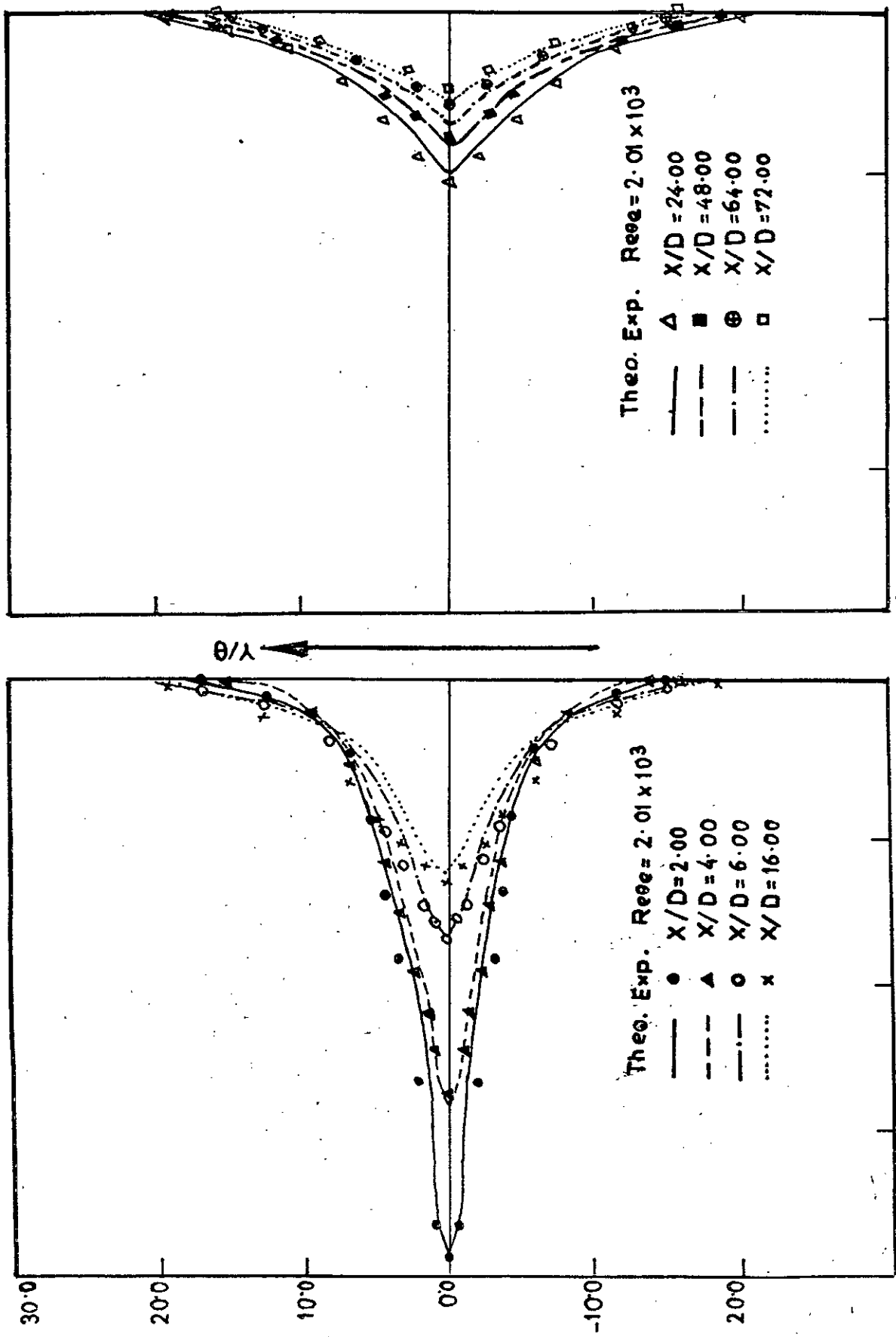

FIG. 4.4.b MEAN VELOCITY DISTRIBUTION IN WAKE

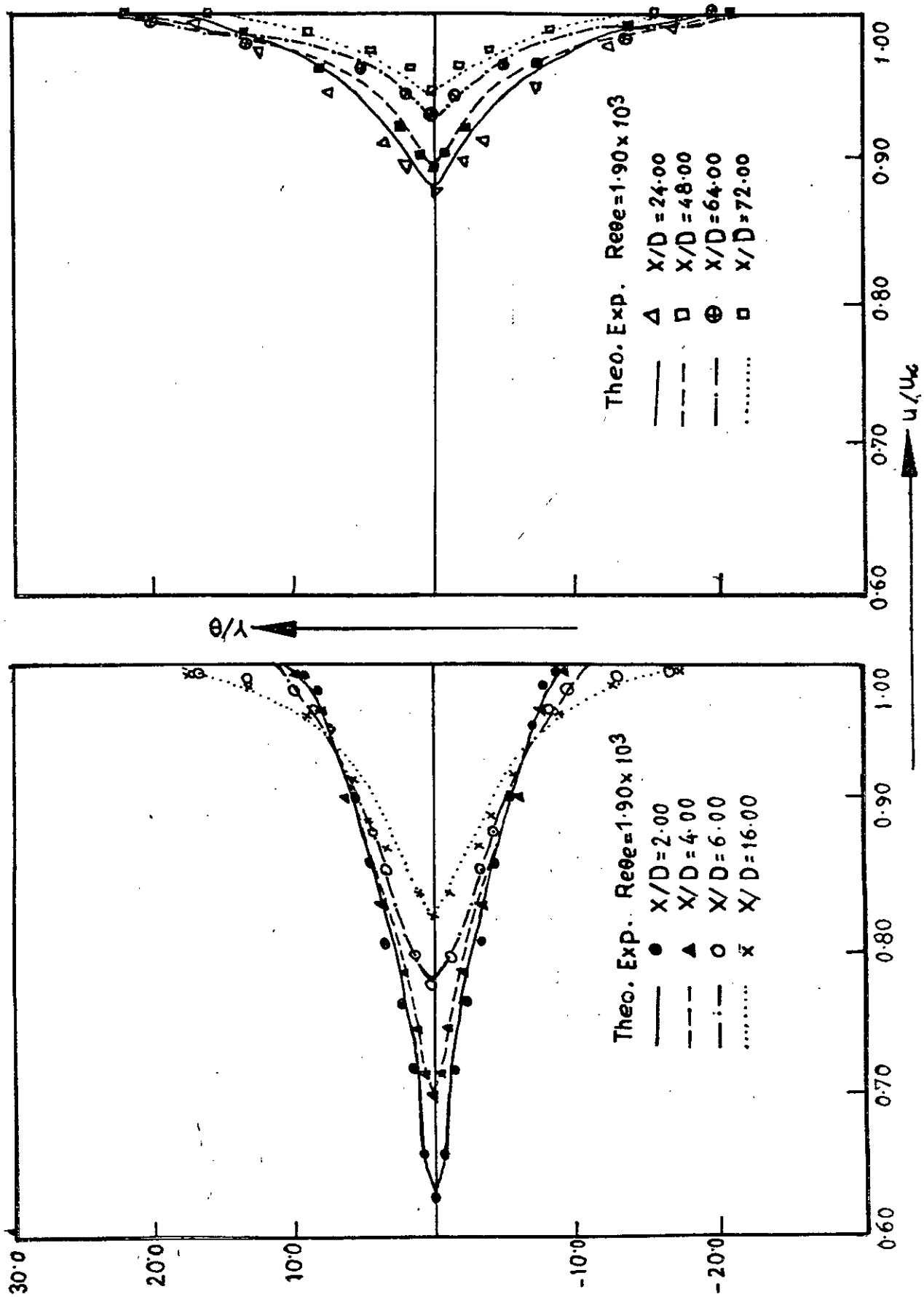

FIG.4.4.C MEAN VELOCITY DISTRIBUTION IN WAKE

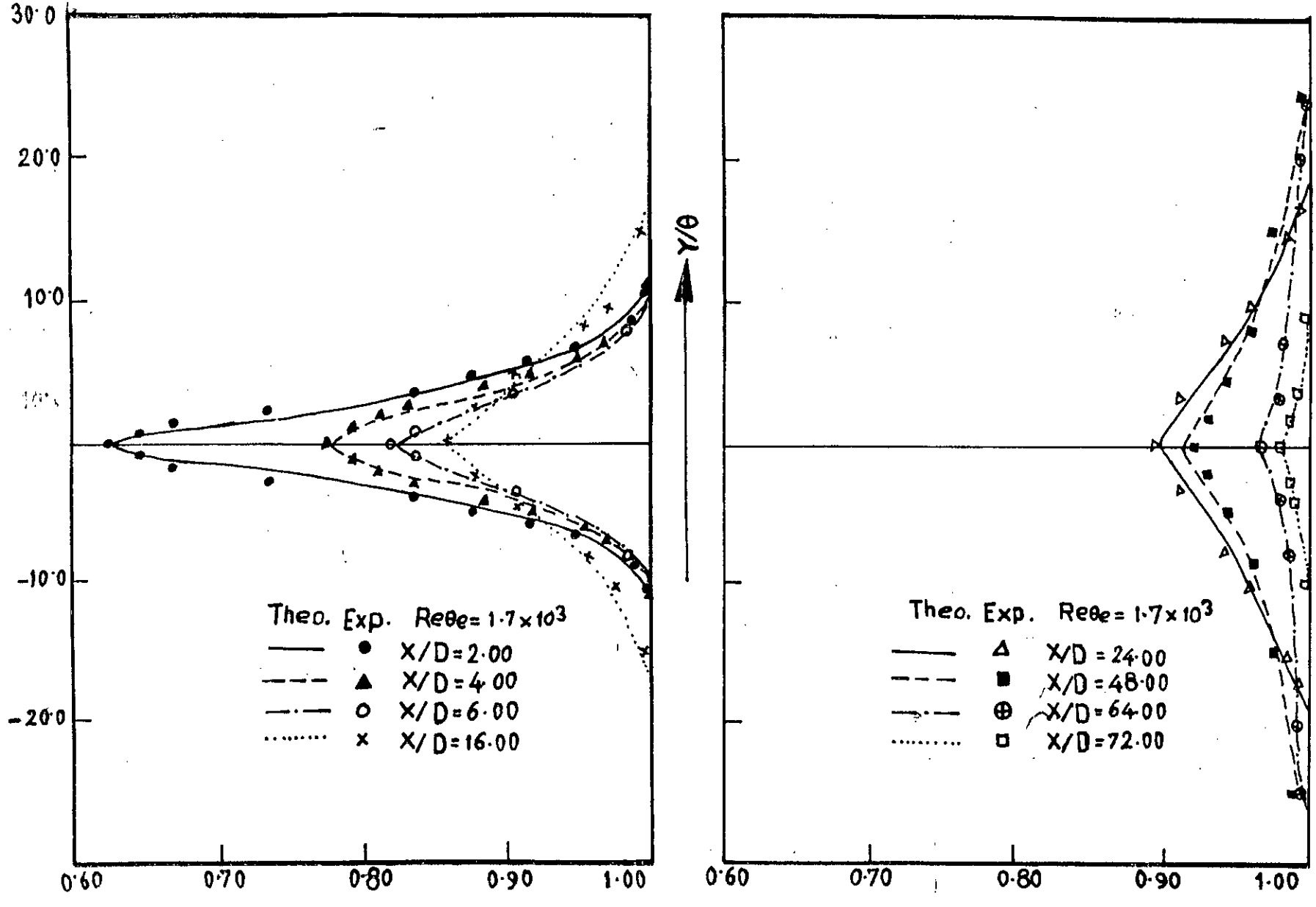

FIG.4·4 d MEAN VELOCITY DISTRIBUTION IN WAKE

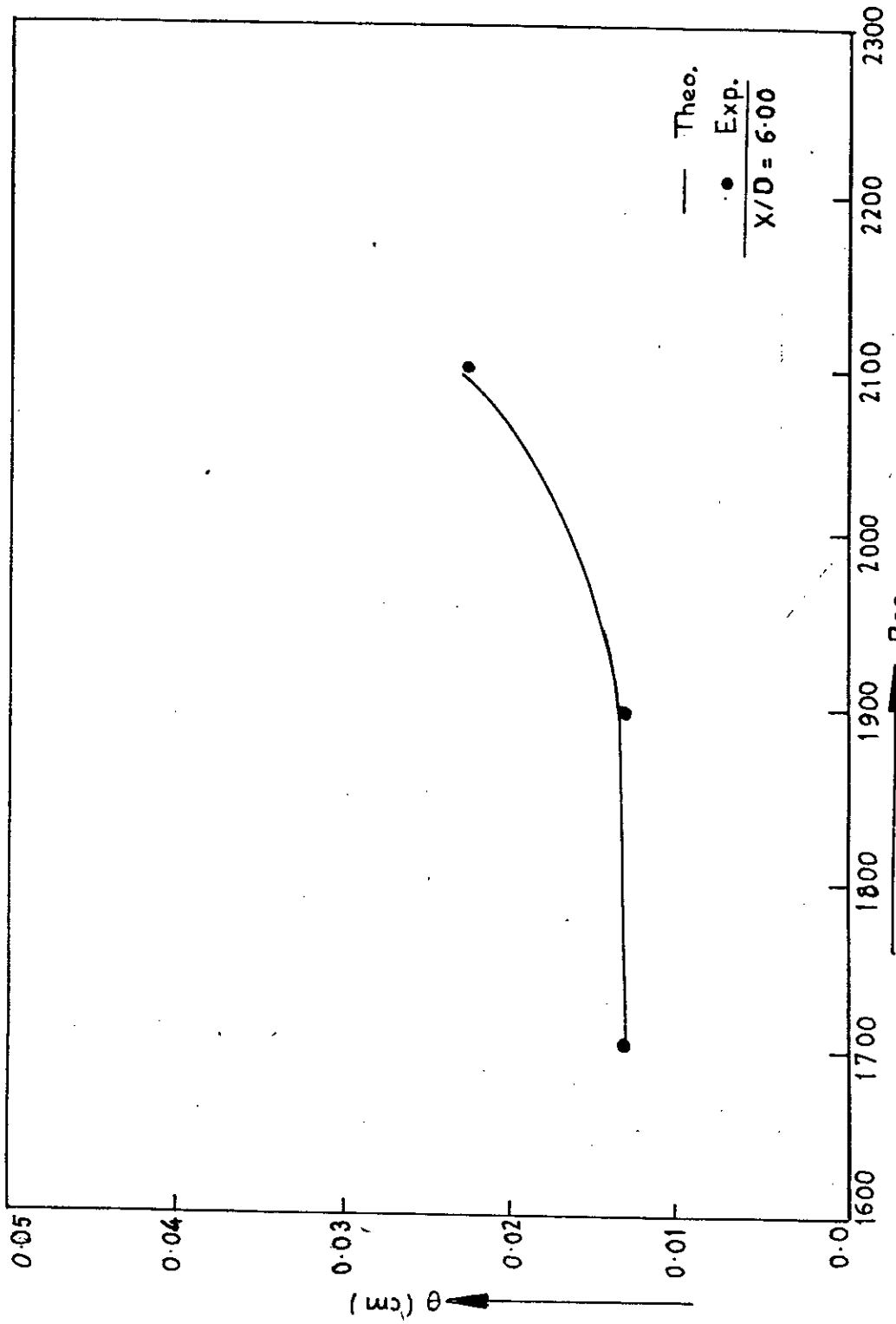

FIG.4.5 VARIATION OF WAKE MOMENTUM THICKNESS WITH REYNOLDS NUMBER

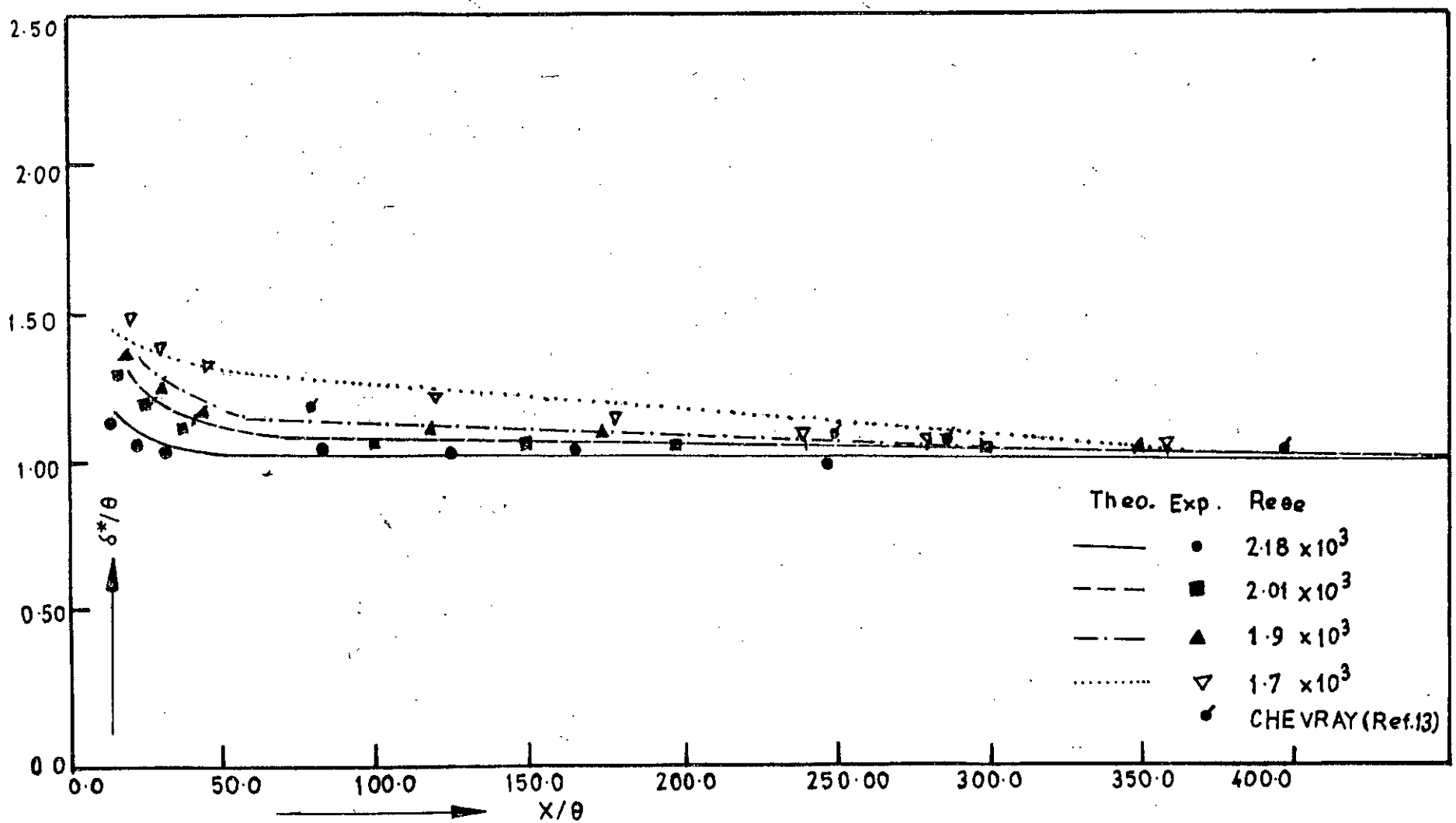

FIG. 4·6 VARIATION OF SHAPE PARAMETERS WITH AXIAL DISTANCE

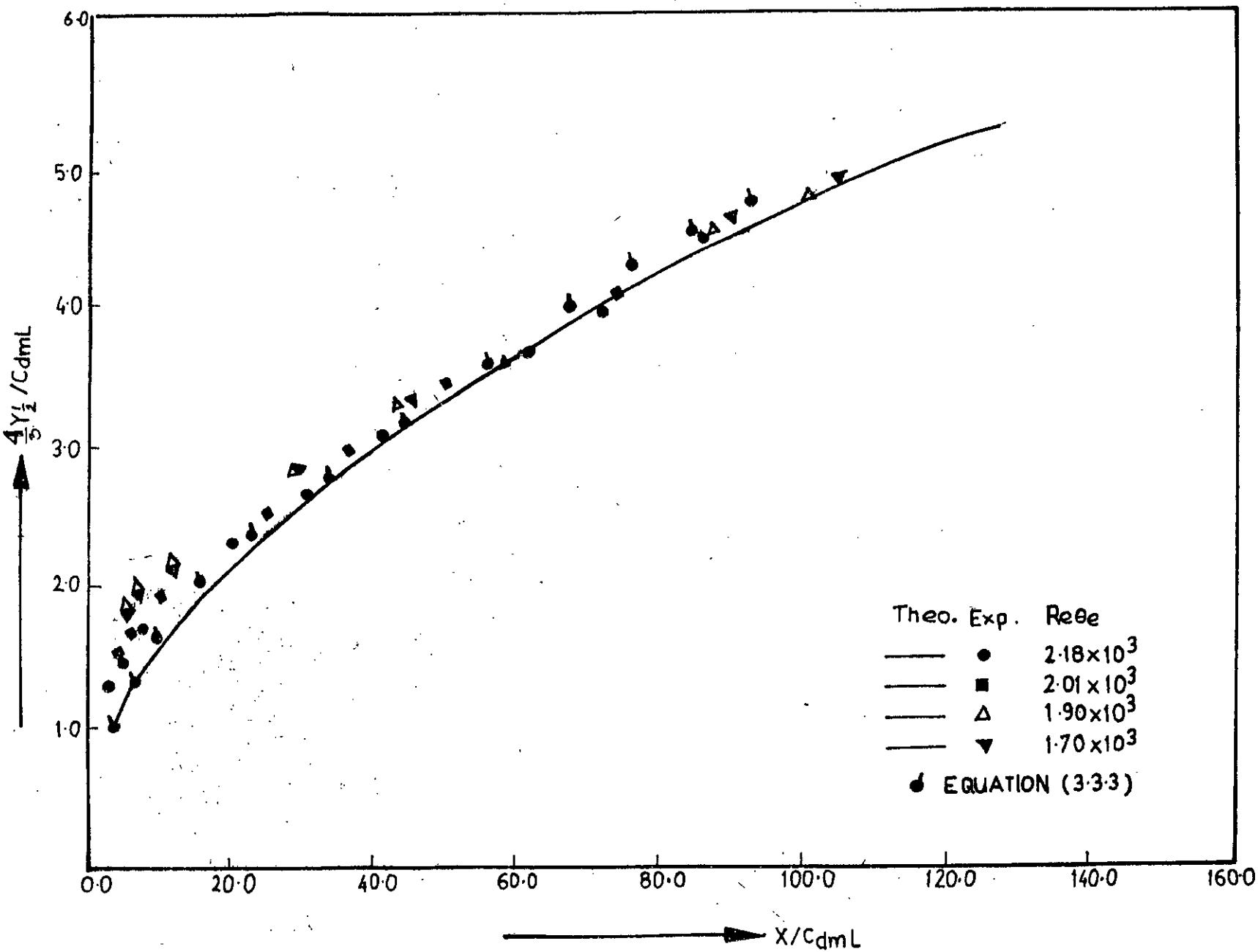

FIG. 47 DIMENSIONLESS HALF VELOCITY LINE AT VARIOUS DISTANCES FROM THE PLATE

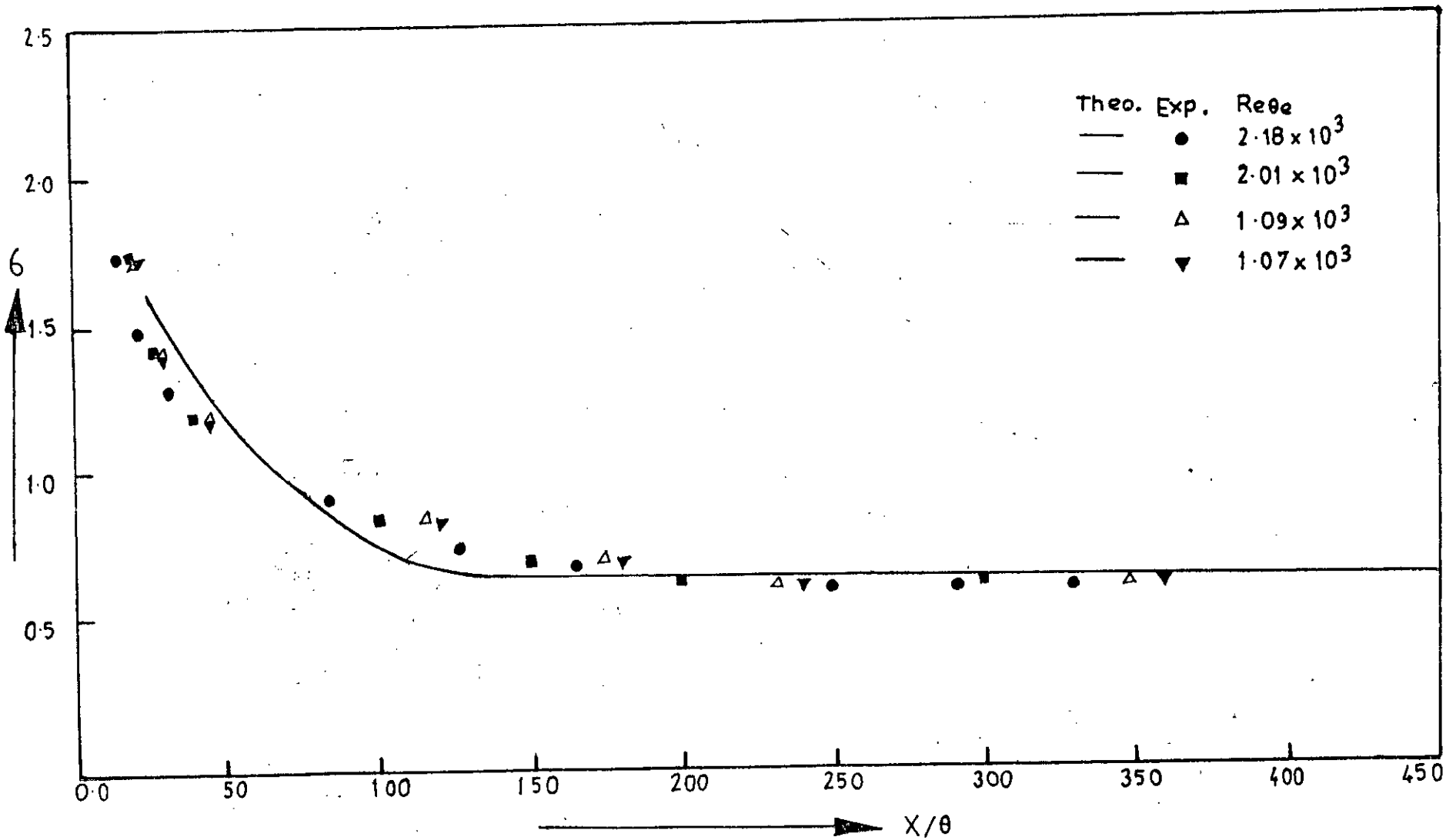

FIG. 4.8 VARIATION OF SPREAD PARAMETER WITH AXIAL DISTANCE

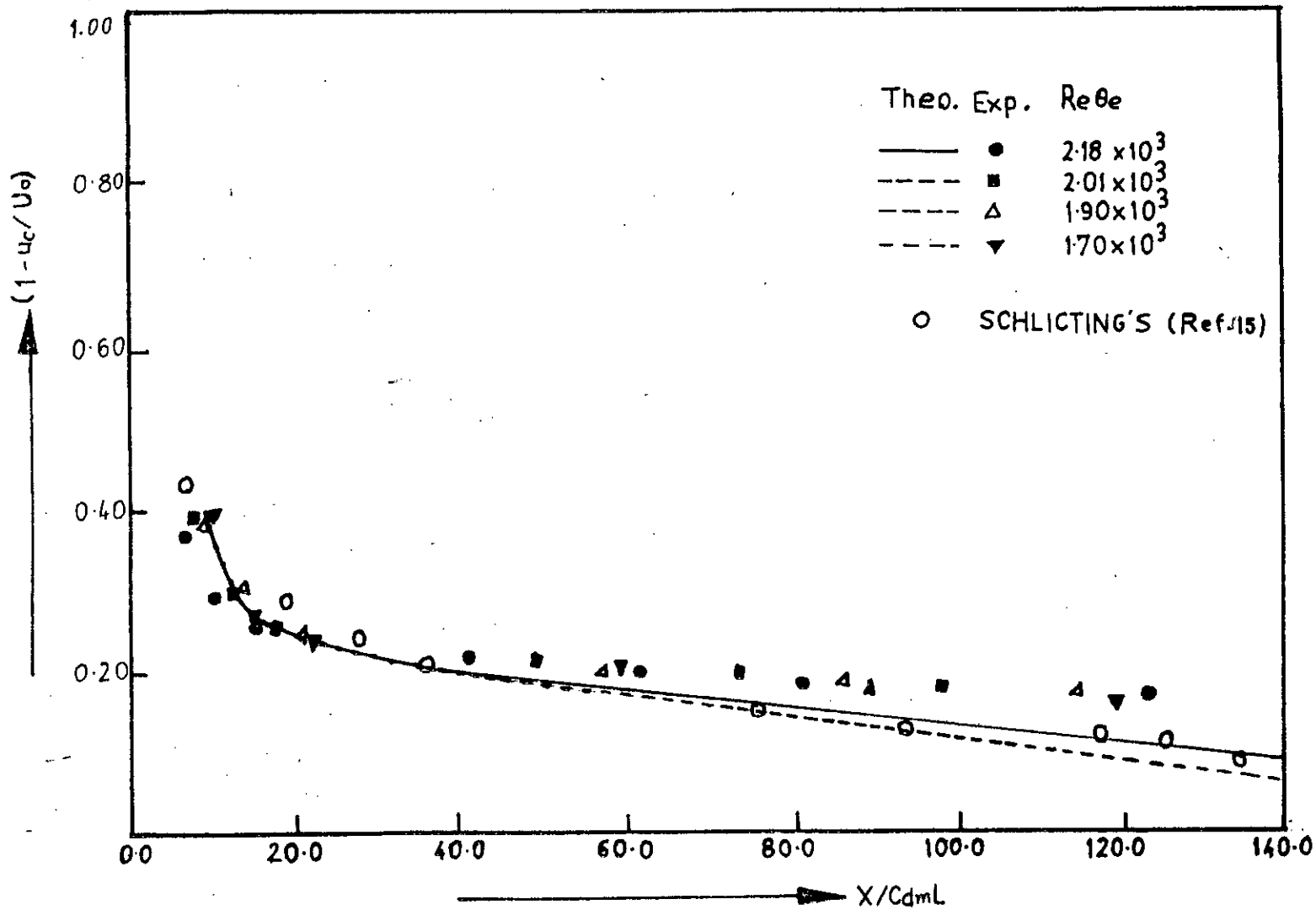

FIG. 4.9 VARIATION OF RELATIVE VELOCITY DEFECT WITH THE AXIAL DISTANCE

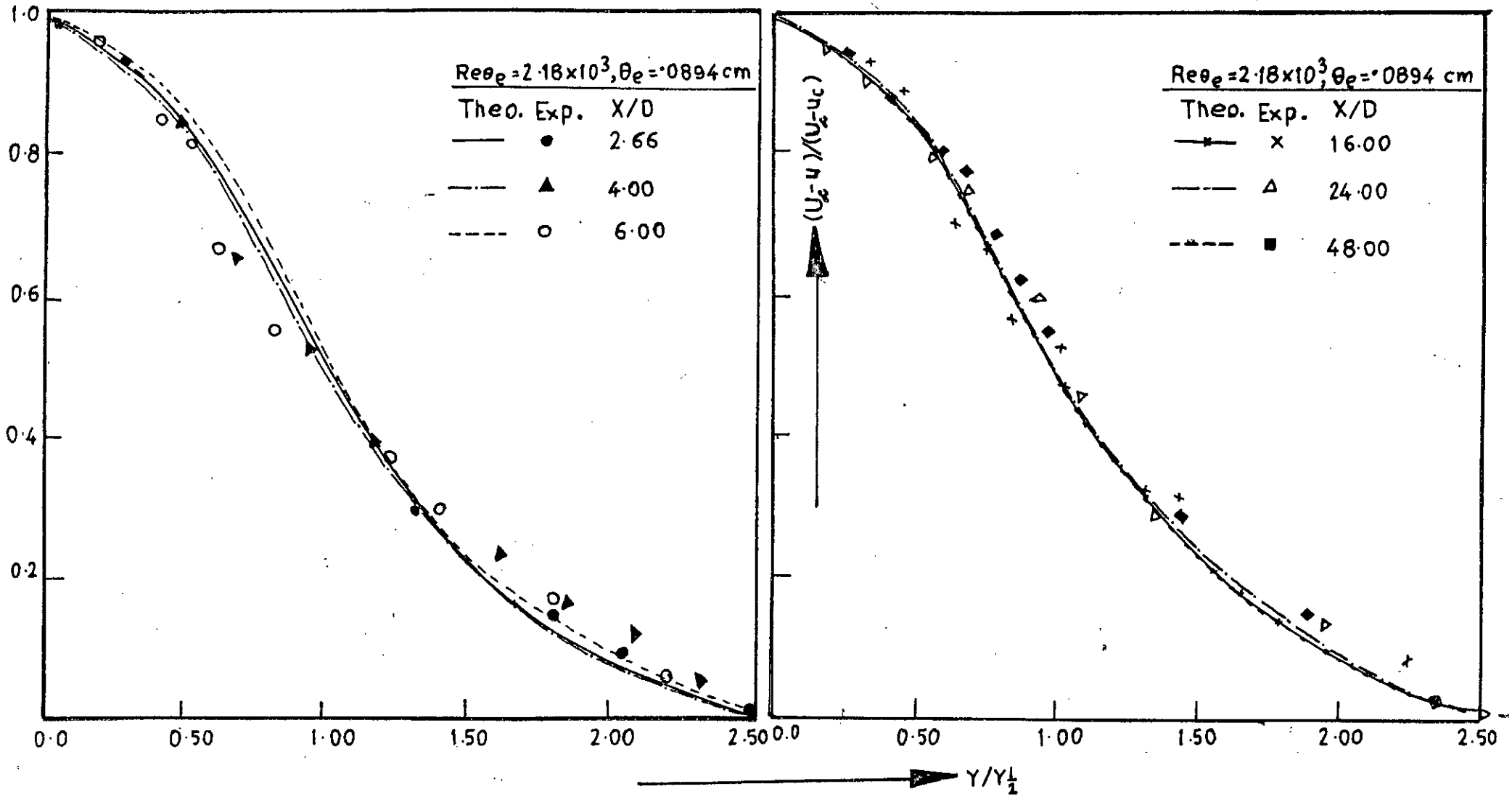

FIG. 4·10a DIMENSIONLESS VELOCITY PROFILE IN THE WAKE OF A FLAT PLATE

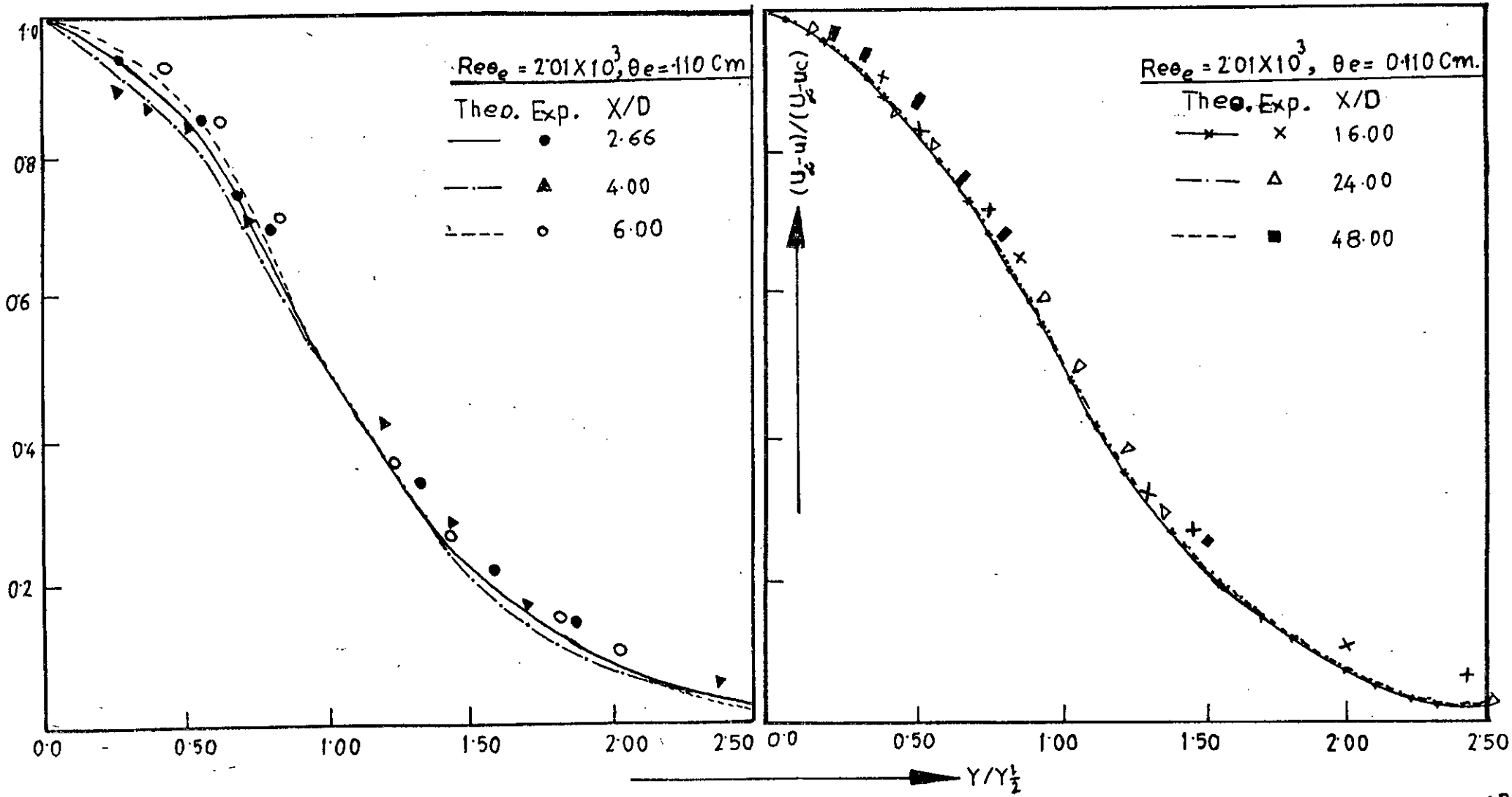

FIG·4.10b DIMENSIONLESS VELOCITY PROFILE IN THE WAKE OF A FLAT PLATE

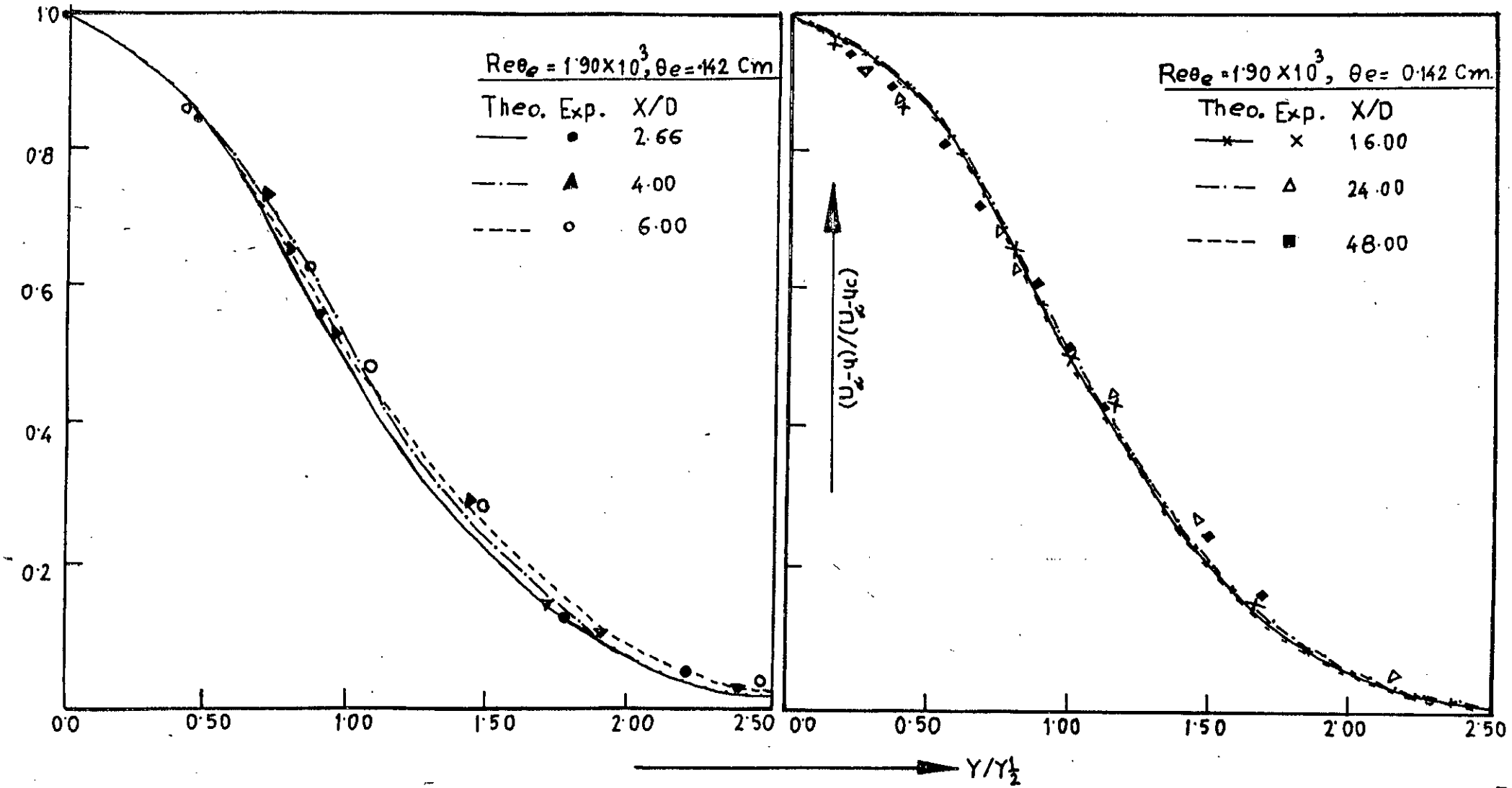

FIG·4.10c DIMENSIONLESS VELOCITY PROFILE IN THE WAKE OF A FLAT PLATE

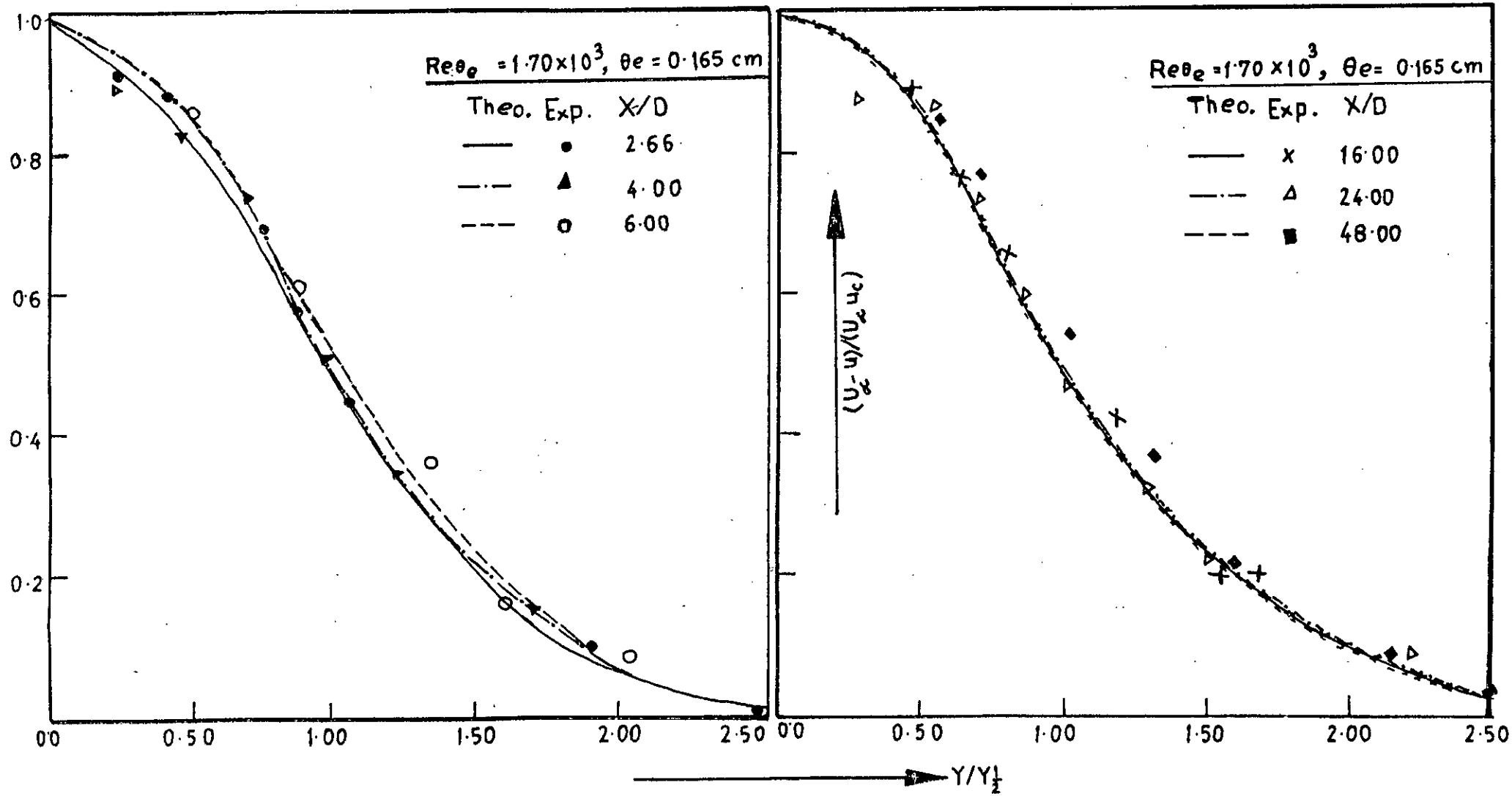

FIG.4.10 d. DIMENSIONLESS VELOCITY PROFILE IN THE WAKE OF A FLAT PLATE

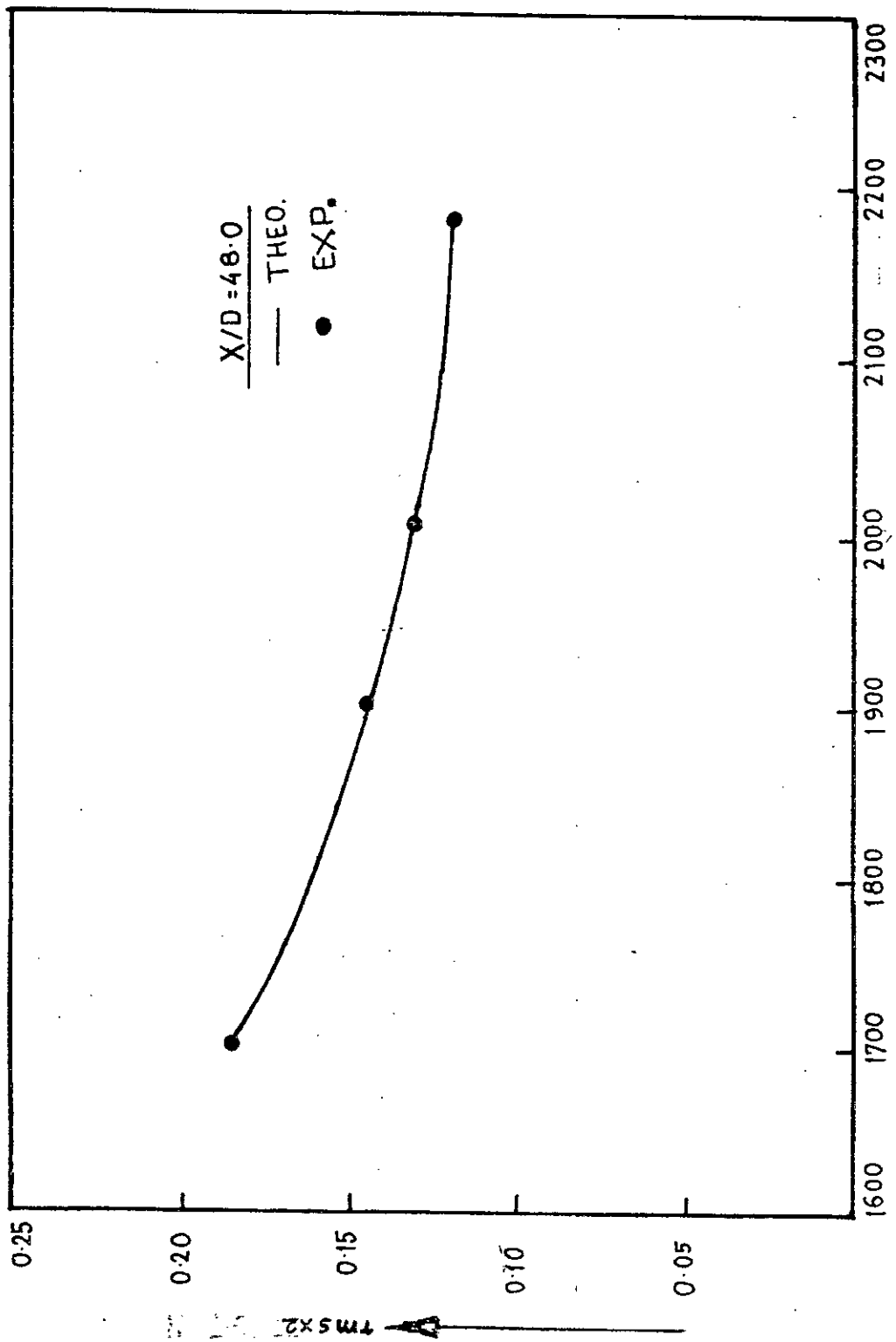

FIG. 4·11 VARIATION OF rms DEVIATION WITH REYNOLDS NUMBER

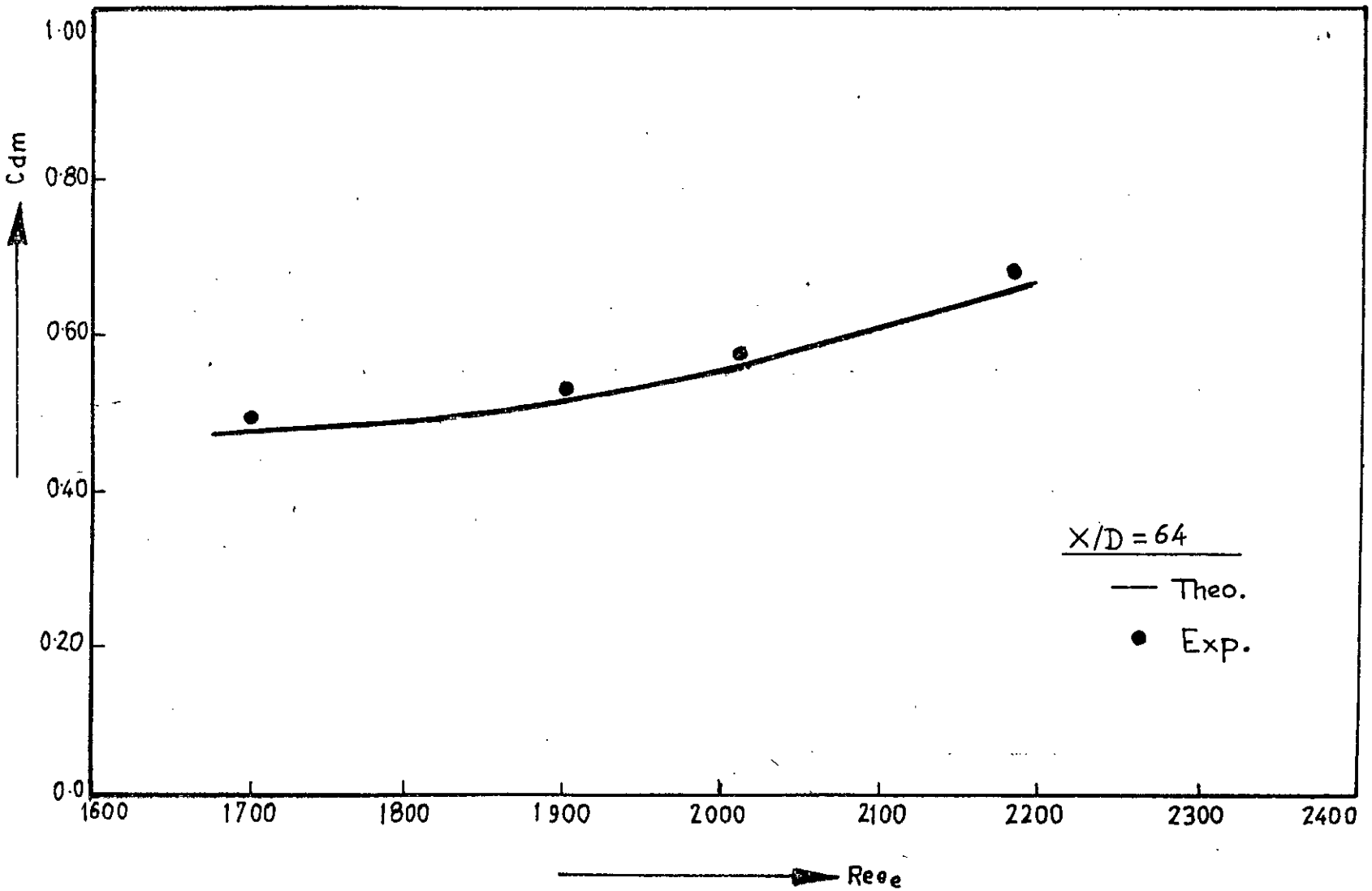

FIG. 4·12 VARIATION OF DRAG-COEFFICIENT WITH REYNOLDS NUMBER

A P P E N D I C E S

APPENDIX - A

DERIVATION OF EQUATIONS

A.1 Differential Equations

The continuity and momentum conservation equations in rectangular system of Co-ordinate for a fluid in motion can be written in terms of shear Stress as

$$\frac{d\rho^{o}}{dt^{o}} + \frac{du^{o}}{dx} + \frac{dv^{o}}{dy} + \frac{dw^{o}}{dz} = 0 \qquad (A.1)$$

$$\rho\frac{du^{o}}{Dto} = \rho Bx + \frac{d\overset{o}{\sigma}xx}{dx} + \frac{d\overset{o}{\sigma}xy}{dy} + \frac{d\overset{o}{\sigma}zx}{dz} \quad \text{x-component} \qquad (A.2a)$$

$$\rho\frac{Dv^{o}}{Dto} = \rho By + \frac{d\overset{o}{\sigma}xy}{dx} + \frac{d\overset{o}{\sigma}yy}{dy} + \frac{d\overset{o}{\sigma}yz}{dz} \quad \text{y-component} \qquad (A.2b)$$

$$\rho\frac{Dw^{o}}{Dto} = \rho Bz + \frac{d\overset{o}{\sigma}zx}{dx} + \frac{d\overset{o}{\sigma}yz}{dy} + \frac{d\overset{o}{\sigma}zz}{dz} \quad \text{z-component} \qquad (A.2c)$$

where, u^{o}, v^{o} and w^{o} are instantaneous velocity components in x,y and z direction respectively. And Bx, By and Bz are the body forces per unit mass along the x,y and z direction, respectively.

Reynolds equation of motion for turbulent flow dissociates instantaneous variables into mean and fluctuating components:

$$
\left.
\begin{aligned}
u^{o} &= u+u' \\
v^{o} &= v+v' \\
w^{o} &= w+w' \\
\overset{o}{\sigma}_{xx} &= \sigma_{xx} + \sigma'_{xx} \\
\overset{o}{\sigma}_{yy} &= \sigma_{yy} + \sigma'_{yy} \\
\overset{o}{\sigma}_{zz} &= \sigma_{zz} + \sigma'_{zz} \\
\overset{o}{\sigma}_{xy} &= \sigma_{xy} + \sigma'_{xy} \\
\overset{o}{\sigma}_{yz} &= \sigma_{yz} + \sigma'_{yz} \\
\overset{o}{\sigma}_{zx} &= \sigma_{zx} + \sigma'_{zx} \\
\overset{o}{p} &= p+p' \\
t^{o} &= t+t'
\end{aligned}
\right\} \qquad (A.3)
$$

where, $u, v, w, \sigma_{xx}, \sigma_{yy}, \sigma_{zz}, \sigma_{xy}, \sigma_{yz}, \sigma_{zx}$, p and t are the mean components and u', v', w', σ'_{xx}, σ'_{yy}, σ'_{zz}, σ'_{xy}, σ'_{yz}, σ'_{xx}, p' and t' are the fluctuating components. The time averages are formed at a fixed point in space and are given, e.g. by

$$u = 1/t_1 \int_{t=to}^{t^{o}+t_1} u\,dt \qquad (A.4)$$

In this connection it is understood that the mean components are taken over a sufficiently long interval of time, t_1, for them to be completely independent of time. Thus by definition, the time-averages of all quantities are equal to zero:

$$\text{i.e.} \quad \overline{u'} = \overline{v'} = \overline{p'} = \overline{f'} = \overline{\sigma'_{xx}} = \overline{\sigma'_{yy}} = \overline{\sigma'_{zz}} = \overline{\sigma'_{xy}} = \overline{\sigma'_{yz}} = \overline{\sigma'_{zx}} = 0$$

$$\text{-----} (A.5)$$

It is useful to list here several rules of operating time- averages as they will be required for reference. If f and g are two dependent variables whose mean values are to be formed and if s denotes any one of the independent variables x,y,z and t then the following rules apply:

$$\left.\begin{aligned} &\bar{\bar{f}}=\bar{f} \\ &\overline{f+g}=\bar{f}+\bar{g} \\ &\overline{\bar{f}.g}=\bar{f}.\bar{g} \\ &\overline{u^2}=\bar{u}^2+\overline{u'^2} \\ &\overline{\frac{df}{ds}}=\frac{d\bar{f}}{ds} \end{aligned}\right\} \qquad (A.6)$$

Introducing equation (A.3) in equation (A.1) and considering steady state

$$\frac{d}{dx}(u+u') + \frac{d}{dy}(v+v') + \frac{d}{dz}(w+w')=0 \qquad (A.7)$$

Taking time-average

$$\frac{du}{dx} + \frac{dv}{dy} + \frac{dw}{dz} = 0 \qquad (A.8)$$

For two-dimensional case $\frac{dw}{dz} = 0$, so the mean flow continuity equation for two dimensions is

$$\frac{du}{dx} + \frac{dv}{dy} = 0 \qquad (A.9)$$

Again from (A.2a) we get

$$\rho\frac{Du}{Dt} = \rho\left[\frac{du}{dt} + u^{o}\frac{du^{o}}{dx} + v^{o}\frac{du^{o}}{dy} + w^{o}\frac{du^{o}}{dz}\right] = \rho Bx + \frac{d}{dx}\sigma^{o}_{xx} + \frac{d}{dy}\sigma^{o}_{xy} + \frac{d}{dz}\sigma^{o}_{zx}$$

$$\text{or,}\quad \rho\frac{du}{dt} = \rho Bx + \frac{d}{dx}(\sigma^{o}_{xx} - u^{o2}) + \frac{d}{dy}(\sigma^{o}_{xy} - \rho u^{o}v^{o}) + \frac{d}{dz}(\sigma^{o}_{zx} - \rho v^{o}w^{o}) \qquad (A.10)$$

Now introducing equation(A.3) into(A.9) we get

$$\rho\frac{d}{dt}(u+u') = \rho Bx + \frac{d}{dx}\left[(\sigma_{xx} + \sigma'_{xx}) - (u+u')^{2}\right] + \frac{d}{dy}\left[(\sigma_{xy} + \sigma'_{xy}) - (u+u')(v+v')\right] + \frac{d}{dz}\left[(\sigma_{zx} + \sigma'_{zx}) - (u+u')(w+w')\right] \qquad (A.11)$$

Time averaging equation(A.11)

$$\rho\frac{du}{dt} = \rho Bx\ \frac{d}{dx}\left[\sigma_{xx} - \rho(u^{2} + \overline{u'^{2}})\right] + \frac{d}{dy}\left[\sigma_{xy} - \rho(uv + \overline{u'v'})\right] + \frac{d}{dz}\left[\sigma_{zx} - \rho(uw + \overline{u'w'})\right]$$

$$\text{or,}\quad \rho\left[\frac{du}{dt} + u\frac{du}{dx} + v\frac{du}{dy} + w\frac{du}{dz}\right] = \rho Bx + \frac{d}{dx}(\sigma_{xx} - \overline{u'^{2}}) + \frac{d}{dy}(\sigma_{xy} - \rho\overline{u'v'}) + \frac{d}{dz}(\sigma_{xz} - \rho\overline{u'w'})$$

------- (A.12)

APPENDIX - B

FINITE DIFFERENCE FORMULATION

B.1 General

A standard explicit finite difference technique requires very small streamwise steps to satisfy the stability criterion. The finite difference problems domain is made into a net of points as indicated in Fig.3.1 by lettering H_1 and H_2 be small increments of the Co-ordinates x and y. Here the finite difference equations will be written in a form that will be applicable for uneven grid spacings in x and y directions. The dependent variables are expanded in Taylor series, The basic variables are made non-dimensional by using the following transformation:

$$X=xu_\infty/\nu \quad y=yu_\infty/\nu \quad u=u/u_\infty \quad v=v/u_\infty \qquad (B.1.1)$$

Replacing shear stress, τ/ρ by $\chi^2 y^2 \left(\frac{du}{dy}\right)^2$, then the final differential from of the continuity and momentum equations are

$$\frac{dU}{dx}+\frac{dV}{dy}=0 \qquad (B.1.2)$$

$$\frac{UdU}{dx}+\frac{VdU}{dy}=2\chi^2\left[Y\left(\frac{dU}{dx}\right)^2+Y^2\left(\frac{dU}{dy}\right)\left(\frac{d^2U}{dy^2}\right)\right] \qquad (B.1.3)$$

B.2 Finite Difference Equations

Taylor's expansion about grid in x-and y-directions

$$X=(I-1)H_1 \qquad (B.2a)$$

$$Y=(J-1)H_2 \qquad (B.2b)$$

$$U=U(I,J) \tag{B.2c}$$

$$V=V(I,J) \tag{B.2d}$$

By forward difference method

$$\frac{dU}{dy} = \left[U(I,J+1)-U(I,J)\right]/H_2 \tag{B.2.5}$$

$$\frac{dU}{dx} = \left[U(I+1,J)-U(I,J)\right]/H_1 \tag{B.2.6}$$

$$\frac{dV}{dy} = \left[V(I,J+1)-V(I,J)\right]/H_2 \tag{B.2.7}$$

$$\frac{dV}{dx} = \left[V(I,J+1)-(I,J)\right]/H_1 \tag{B.2.8}$$

$$\frac{d^2U}{dy^2} = \left[U(I,J+2)-2U(I,J+1)+U(I,J)\right]/2H_2^2 \tag{B.2.9}$$

By backward difference method

$$\frac{dU}{dy} = \left[U(I,J)-U(I,J-1)\right]/H_2 \tag{B.2.10}$$

$$\frac{dU}{dx} = \left[U(I,J)-U(I-1,J)\right]/H_1 \tag{B.2.11}$$

$$\frac{dV}{dy} = \left[V(I,J)-V(I,J-1)\right]/H_2 \tag{B.2.12}$$

$$\frac{dV}{dx} = \left[V(I,J)-V(I-1,J)\right]/H_1 \tag{B.2.13}$$

By central difference method

$$\frac{dV}{dy} = \left[U(I,J+1)-U(I,J-1)\right]/H_2 \tag{B.2.14}$$

$$\frac{dU}{dx} = \left[U(I+1,J)-U(I-1,J)\right]/2H_1 \tag{B.2.15}$$

$$\frac{d^2U}{dy^2} = \left[U(I,J+1)-2U(I,J)+U(I,J-1)\right]/H_2 \tag{B.2.16}$$

B.3 Continuity Equation

Using equations(B.2.6) and (B.2.7) in equation(B.1.2) finite difference form of continuity equation is

$$\left[U(I+1,J)-U(I,J)\right]/H_1+\left[V(I,J+1)-V(I,J)\right]/H_2=0 \qquad (B.3.1)$$

B.4 Momentum equation

Using equations(B.2.1), (B.2.2),(B.2.3),(B.2.4), (B.2.5),(B.2.6),(B.2.8) and (B.2.9) in equation(B.1.3) finite difference form of momentum equation is

$$U(I,J)\left[U(I+1,J)-U(I,J)\right]/H_1+V(I,J)\left[U(I,J+1)-U(I,J)\right]/H_2$$
$$=2\chi^2\left[(J-1)H_2\left[(U(I,J+1)-U(I,J))/H_2\right]^2\right.$$
$$+(J-1)^2H_2^2\left[(U(I,J)-U(I,J-1))/H_2\right]\left[(U(I,J+2)-\right.$$
$$\left.\left.2U(I,J+1)+U(I,J))/2H_2^2\right]\right] \qquad (B.4.1)$$

APPENDIX - C

METHODOLOGY FOR DETERMINING POWER INDEX 'n' IN INITIAL VELOCITY PROFILE

The initial velocity profile given by Prandtl for turbulent flow [15]

$$u/u_{\infty} = (y/\delta)^{1/n} \qquad (C.1)$$

where, $\delta = \delta(x)$ is the thickness of the boundary layer.

The empirical integral equation of momentum thickness is:

$$\theta = \int_0^{\infty} u/u_{\infty}\,(1-u/u_{\infty})\,dy \qquad (C.2)$$

where, θ is called the momentum thickness of the wake. The 'n' can be determined from the equation(C.2) for the limiting value 0 to δ i.e.

$$\frac{\theta}{\delta} = \frac{1}{\delta}\int_0^{\delta} \frac{u}{u_{\infty}}\left(1-\frac{u}{u_{\infty}}\right) dy \qquad (C.3)$$

Putting the equation(C.1) in to (C.3) the equation(C.3) becomes

$$\frac{\theta}{\delta} = \frac{1}{\delta}\int_0^{\delta}\left[(y/\delta)^{\frac{1}{n}} - (y/\delta)^{\frac{2}{n}}\right] dy \qquad (C.4)$$

after integrating

$$\frac{\theta}{\delta} = n/(n^2+3n+2)$$

or, $$n = \tfrac{1}{2}\left[\left(\frac{\delta}{\theta}-3\right) \pm \sqrt{\left(\frac{\delta}{\theta}-3\right)^2-8}\right] \qquad (C.5)$$

where, $\frac{\delta}{\theta}$ is found from experimental results of Ref. [8] (Table 4.1)

APPENDIX - D

ANALYSIS OF DIFFERENT SHEAR STRESS MODELS

Boussinesq [3] was first to work on turbulent flow shear stress. He introduced a mixing Co-efficient, A_τ, for the Reynolds stress in turbulent flow by putting

$$\tau_t = \rho\overline{u'v'} = A_\tau \frac{du}{dy} \qquad (D.1)$$

where, A_τ is the turbulent mixing Co-efficient. The eddy kinematic viscosity can be expressed as

$$\varepsilon_\tau = A_\tau / \rho \qquad (D.2)$$

So the turbulent shear stress becomes

$$\tau_t = \rho \varepsilon_\tau \frac{du}{dy} \qquad (D.3)$$

The Boussinesq model can not be used in practic as nothing is known about the dependence of A_τ on velocity.

Habib and Whitelaw [7] worked on turbulent energy flow and gave the shear stress model

$$\tau_t = \rho c_\mu k/\varepsilon \left(\frac{du}{dy}\right) \qquad (D.4)$$

where, c_μ is the viscosity constant, K is the kinetic energy and ε is the turbulent energy dissipation rate. This model is applicable only for fully developed turbulent flow. Numerical results were in close agreement with experimental results.

Prandtl [4] deduced a kinetc energy model (K)

$$\tau_t = \rho c_\mu k^{1/2} \left(\frac{du}{dy}\right) \qquad (D.5)$$

where, $\ell = \lambda_s Y_G$, λ_s is the proportionality constant and Y_G is the effective width of shear flow. This model is used for turbulent wakes and jets, gives better performance.

In order to develop the preceding method(Initiated by Bossinesq [3]), it is necessary to find empirical relations between the Co-efficients and the mean velocity. In 1925 Prandtl [4] made an important advance in this direction. He introduced the mixing length concept in the shear strees equation

$$\tau_t = -\rho \overline{u'v'} = \rho \ell^2 \left(\frac{du}{dy}\right)^2 = \rho \ell^2 \left|\frac{du}{dy}\right| \left|\frac{du}{dy}\right| \qquad (D.6)$$

where, ℓ = mixing length.

This is Prandtl's mixing length hypothesis. This model has been successfully applied to the study of turbulent motion along walls (pipe, channel, boundary layer) and to the problem of so called free turbulent flow. (The later term refers to flow without solid walls, such as jets and wakes) This model is used for both developing and developed turbulent profiles. Numerical solution by finite difference method was in close agreement with experimental results of Faruque [8]

Prandtl's [4] equation for shear stress in turbulent flow is still unsatisfactory in that the apparent kinematic viscosity ε_τ, vanishes at points where $\frac{du}{dy}$ is equal to zero i.e. at point of maximum or minimum velocity. In order to counter these difficulties Prandtl [9] defined a considerably simpler equation for the apparent (eddy) kinematic viscosity, given by

$$\varepsilon_\tau = \varkappa b (U_{max} - U_{min})$$

where, χ denotes a dimensionless number to be determined experimentally and b denotes the width of the mixing zone. So the turbulent shearing stress is given by

$$\tau_t = \rho \chi b (U_{max} - U_{min}) \frac{du}{dy} \qquad (D.7)$$

In Prandtl's theory, the assumption is made that the mean velocity remains constant during the transverse motion of a lump of fluid Taylor [10] gave the equation of sheas stress as

$$\tau = \tfrac{1}{2} \rho l_w^2 \left|\frac{du}{dy}\right| \left(\frac{du}{dy}\right) \qquad (D.8)$$

where, $l_w = \sqrt{2}\, l$

Toylor [10] concluded that the diffusions of temperature differences and vorticity in the mixing zone behind a cylinderical rod occur in conformity with identical laws.

It would be very conveient to possess a rule which allow to determine the dependence of mixing length on space Co-ordinetes.

von Kármár [5] made an attempt to establish a relation between mixing length and mean velocity

$$l \sim \left(\frac{du}{dy}\right) / \left(\frac{d^2}{dy^2}\right) \qquad (D.9)$$

By introducing an empirical dimensionless constant von Karmar [5] gets the final form of the equation (D.6) as

$$\tau_t = \rho \chi^2 \left(\frac{du}{dy}\right)^4 \Big/ \left(\frac{d^2u}{dy^2}\right)^2 \qquad (D.10)$$

APPENDIX-E

COMPUTER PROGRAM

```
C   ***************************************************************
C   * FINITE DIFFERENCE SOLUTION OF A WAKE FOR TURBULENT          *
C   * FLOW BEHIND A FLAT PLATE                                    *
C   ***************************************************************
C   * PRANDTL'S MIXING LENTH SHEAR STRESS MODEL                   *
C   * THEGOVERNING EQUATIONS-CONTINUITY AND MOMENTUM FOR          *
C   * TURBULANT FLOW                                              *
C   ***************************************************************
C   * THICKNESS OF THE PLATE=D=1.905CM;EMPIRICAL CONST=0.04       *
C   * TRAILING EDGE FREE STREAM VEL.=U0;EC=0.04*0.04              *
C   * KINIMATIC VISCOSITY=VK=1.33E-05 M2/SEC                      *
C   * MOMENTUM THICKNESS=THETA,RENOLD'S NO.BASE ON THETA=RET      *
C   * BOUNDARY LAYER THICKNESS=DELTA;AVERAGE VEL.=UAV             *
C   * SHEAR VELOCITY=UF                                           *
C   * DIMENSION LESS COMPONENTS:                                  *
C   * MEAN VELOCITY=U/U0;                                         *
C   * AXIAL DISTANCE = X= X/D , XT= X/THETA , XC= X/COML;         *
C   * VERTICAL DISTANCE=Y/THETA ; HALF WIDTH=Y3=Y/Y(I/2)          *
C   ***************************************************************
C   ********************* MAIN PROGRAM ****************************
      DIMENSION U(5,85),U1(80),V(85,85),X(2500),Y(90),DEL(2500)
     +,F(2500),F1(2500),THE(2500),Y3(60),U2(80),XT(2500),
     +YC(2500),CM(2500),SP(2500),SF(2500),DS(2500),XC(2500)
      H1=0.013
      H2=0.07
      K=1
      L=1
      D=1.905
      VK=1.321E-05
      EC=0.16
C*********TABLE FOR TRALING EDGE CONDITION*******************
C   RET  =2180      2013      1900      1700                  *
C   DELTA=0.762     0.985     1.39      1.6       CM          *
C   THETA=0.0894    0.1107    0.1422    0.1651    CM          *
C   UAV  =18.10     13.49     9.99      7.65      M/SEC       *
C   UF   =0.832     0.683     0.509     0.418     M/SEC       *
C***************************************************************
      RET=2180
      DELTA=0.762
      THETA=0.0894
      UAV=18.10
      UF=0.832
C**DETERMINATION OF POWER FACTOR=B
      T=THETA/DELTA
      A=((-3.0+1/T)+SQRT((3-1/T)*(3-1/T)-8.0))/2.0
      B=1/A
C**DETERMINATION OF TRAILING EDGE VEL.DIST.
      N=45
      DO 11 J=1,24
11    U(1,J)=(J*H2/DELTA)**B
```

```
      DO 12 J=1,N
   12 V(J,1)=0.0
    C   RET=2180-2010-1900-1700
    C   JJ= 10    14    19    22
      DO 13 JJ=10,N
   13 U(1,JJ)=0.99
      WRITE(3,4)
    4  FORMAT(1X,35('*$')/2X,'SL.',1X,'|',3X,'U',
     +3X,'|',2X,'UT',4X,'|',2X,'UN',6X,'|',2X,'UP',
     +4X,'|',4X,'Y',3X,'|',2X,'YT',4X,'|',2X,'TH'
     +/1X,35('*$')/)
      DO 14 I=1,N
    C   MEAN VELOCITY=UT M/SEC
      UT=U(1,I)*UAV
      YT1=H2*(I-1)/THETA
    C   VERTICAL HEIGHT=YT CM
      YT=0.10+I*H2
    C   UNIVERSAL LOG VEL.(TRAILING EDGE)UN=UF*Y/KV
      UN=UF*I*H2/(100.0*VK)
      UP=UT/UF
   14 WRITE(3,15)I,U(1,I),UT,UN,UP,YT1,YT,THETA
   15 FORMAT(2X,I2,1X,F8.4,1X,F8.4,1X,F10.3,1X,
     +F8.4,1X,F8.4,1X,F8.3,1X,F8.3)
    C**DETERMINATION OF VEL.DIST.IN THE WAKE*****
   16 L=1
      V(K,L)=0.0
    C   FINITE DIFFERENCE FORM OF DERIVITIVES
   17 DUYF=(U(K,L+1)-U(K,L))/H2
```

360N-FO-479 3-8 MAINPGM DATE 05/05/96 TIME

```
      DUYB=(U(K,L)-U(K,L-1))/H2
      DUY2=(U(K,L+1)-2*U(K,L)+U(K,L-1))/H2
      DYF=DUYF*DUYF
      IF(L.GT.1)GO TO 18
      DUY2F=(U(K,L+2)-2*U(K,L+1)+U(K,L))/(2*H2*H2)
      Y11=L*H2
      Y21=Y11*Y11
    C   FINITE DIFFERENCE FORM OF MOMENTUM EQ.(GRID-1)
      U(K+1,L)=(((2.0*EC*(Y11*DYF+Y21*DUYF*DUY2F))-V(K,L)
     +*DUYF)/U(K,L))*H1+U(K,L)
      DUXF=(U(K+1,L)-U(K,L))/H1
    C   FINITE DIFFERENCE FORM OF COMTINUITY EQ.(GRID-1)
      V(K,L+1)=V(K,L)-DUXF*H2
      GO TO 19
   18 Y1=(L-1)*H2
      Y2=Y1*Y1
    C   FINITE DIFFERENCE FORM OF MOMENTUM EQ.(GRID.GT.1)
      U(K+1,L)=(((2.0*EC*(Y1*DYF+Y2*DUYB*DUY2F))-V(K,L)
     +*DUYF)/U(K,L))*H1+U(K,L)
      DUXB=(U(K,L)-U(K-1,L))/H1
      DUXF=(U(K+1,L)-U(K,L))/H1
    C   FINITE DIFFERENCE FORM OF CONTINUITY EQ.(GRID.GT.1)
      V(K,L+1)=V(K,L)-DUXF*H2
   19 KK=K+1
      IF(U(KK,L)-0.99)20,21,21
   20 L=L+1
      GO TO 17
   21 U(KK,L)=0.99
    C   BOUNDARY LAYER THICKNESS=DEL
```

```
      DEL(K)=L*H2
C     DETERMINATION OF MOMENTUM THICKNESS AND SHAPE FACTOR
      F(1)=0.0
      F1(1)=0.0
      DO 22 M=1,L
   22 F(M+1)=F(M)+(U(K+1,M)*(1-U(K+1,M))*H2)
      F1(M+1)=F1(M)+(1-U(K+1,M))*H2
C     MOMENTUM THICKNESS=THE
      THE(KK)=F(L)
      DS(KK)=F1(L)
C     SHAPE FACTOR=SF
      SF(KK)=DS(KK)/THE(KK)
      DO 23 LL=L,N
      U(KK,LL)=0.99
      DUXLF=(U(KK,LL)-U(K,LL))/H1
   23 V(K,LL+1)=V(K,LL)-DUXLF*H2
      DO 24 J=1,N
      U(K,J)=U(K+1,J)
   24 V(K-1,J+1)=V(K,J+1)
      X(K)=(5.0+K*H1)/D
      IF(X(K).GT.2.659.AND.X(K).LT.2.67)GO TO 70
      IF(X(K).GT.4.02.AND.X(K).LT.4.04)GO TO 70
      IF(X(K).GT.6.0.AND.X(K).LT.6.0172)GO TO 70
      IF(X(K).GT.16.050.AND.X(K).LT.16.07)GO TO 70
      IF(X(K).GT.23.98.AND.X(K).LT.24.00)GO TO 70
      IF(X(K).GT.48.00.AND.X(K).LT.48.05)GO TO 70
      IF(X(K).GT.64.0.AND.X(K).LT.64.1)GO TO 70
      IF(X(K).GT.71.99.AND.X(K).LT.72.17)GO TO 70
      IF(X(K).ST.72.17)GO TO 80
      IF(X(K).GT.2.67.AND.X(K).LT.4.05)GO TO 25
      GO TO 26
C     RET=2180       2010      1900     1700
C     H1 =0.032      0.032     0.032    0.032
C     H2 =0.040      0.040     0.040    0.040
   25 H1=0.033
      H2=0.04
   26 IF(X(K).GT.4.05.AND.X(K).LT.6.017)GO TO 27
      GO TO 28
C     RET=2180       2010      1900      1700
C     H1 =0.0365     0.0365    0.0365    0.0365
C     H2 =0.02       0.02      0.02      0.02
   27 H1=0.0365
      H2=.02
   28 IF(X(K).GT.6.017.AND.X(K).LT.16.06)GO TO 29
      GO TO 30
C     RET=2180       2010      1900     1700
C     H1 =0.0366     0.0366    0.0366   0.0366
C     H2 =0.20       0.20      0.20     0.20
   29 H1=0.0366
```

360N-FO-479 3-8 MAINPGM DATE 05/05/86 TIME

```
      H2=0.2
   30 IF(X(K).GT.16.06.AND.X(K).LT.24.0)GO TO 31
      GO TO 32
C     RET=2180      2010      1900      1700
C     H1 =0.05      0.05      0.05      0.05
C     H2 =0.20      0.20      0.20      0.20
```

```
31 H1=0.05
   H2=0.2
32 IF(X(K).GT.24.00.AND.X(K).LT.48.05)GO TO 33
   GO TO 34
C  RET=2180     2010     1900     1700
C   H1=0.10     0.10     0.10     0.10
C   H2=0.12     0.12     0.12     0.12
33 H1=.1
   H2=0.12
34 IF(X(K).GT.48.05.AND.X(K).LT.64.1)GO TO 35
   GO TO 36
C  RET=2180    2010     1900     1700
C  H2 =0.10    0.10     0.10     0.10
C  H2 =0.12    0.12     0.12     0.12
35 H1=.1
   H2=0.12
36 IF(X(K).GT.64.1.AND.X(K).LT.72.2)GO TO 37
   GO TO 38
C  RET=2180    2010     1900     1700
C  H1 =0.10    0.10     0.10     0.10
C  H2 =0.12    0.12     0.12     0.12
37 H1=.1
   H2=0.12
38 K=K+1
   GO TO 16
70 WRITE(3,5)
5  FORMAT(1X,58('*$')/3X,'SL.',4X,'|',2X,'U',5X,'|'
  +,4X,'U1',2X,'|',2X,'U2',3X,'|',1X,'X',4X,'|',2X,
  +'Y',4X,'|',2X,'THE',3X,'|',3X,'XT',3X,'|',2X,
  +'Y3',2X,'|',3X,'XC',2X,'|',2X,'YC',2X,'|',2X,'CM'
  +,3X,'|',2X,'SP'/1X,58('*$')/)
   XT(K)=(5.0+K*H1)/THE(KK)
   XC(K)=(5.0+K*H1)/(4.0*THE(KK))
   DO 71 L=1,N
   LL=L+1
   K1=K-1
   CM(K)=4.0*THE(KK)/D
C  DIMENSION LESS MEAN VEL.=U1=(U&-U)/(U&-UC)
   U1(L)=(0.99-U(K,L))/(0.99-U(K,1))
C  DIMENSION LESS RELATIVE CENTER LINEVEL.=U2=(1-UC/U0)
   U2(L)=1.0-U(K,1)/0.99
   IF(U1(L).LE.0.0)GO TO 2
   Y3(L)=SQRT(ABS((-1/ALOG(2.0))*ALOG(U1(L))))
C  SPREAD PARAMETER=SP
   IF(Y3(L).LE.0.0)GO TO 2
   SP(K)=-ALOG(U1(L))/(Y3(L)**2.0)
C  DIMENSION LESS HALF WIDTH VELOCITY=YC=4Y(1/2)/3CDML
2  YC(L)=0.35*SQRT(XT(K))
C  DIMENSION LESS VERTICAL DIST.=Y=Y/THE
   Y(L)=H2*(L-1)/THE(K)
   WRITE(3,90)K,L,U(K,L),U1(L),U2(L),X(K),Y(L),
  +THE(K),XT(K),Y3(L),XC(K),YC(L),CM(K),SP(K)
90 FORMAT(2X,I4,1X,I2,2X,G10.5,1X,F6.3,1X,F6.3,1X,
  +F8.4,1X,F6.3,1X,F8.5,1X,F8.3,1X,F6.3,1X
  +,F8.3,1X,F6.3,1X,F6.4,1X,F6.4)
71 CONTINUE
   K=K+1
   GO TO 16
80 STOP
C  DEBUG INIT
   END
```